RESEARCH ARTICLE

Loss of WNT4 in the gubernaculum causes unilateral cryptorchidism and fertility defects

Abhishek Seth[1,2,3], Juan C. Bournat[1], Olga Medina-Martinez[1], Armando Rivera[2], Joshua Moore[2], Hunter Flores[1], Jill A. Rosenfeld[4,5], Liya Hu[6] and Carolina J. Jorgez[1,2,*]

ABSTRACT

Undescended testis (UDT) affects 6% of male births. Despite surgical correction, some men with unilateral UDT may experience infertility with the contralateral descended testis (CDT) showing no A-dark spermatogonia. To improve our understanding of the etiology of infertility in UDT, we generated a novel murine model of left unilateral UDT. Gubernaculum-specific *Wnt4* knockout (KO) mice (*Wnt4*-cKO) were generated using retinoic acid receptor β2-*cre* mice and were found to have a smaller left-unilateral UDT. *Wnt4*-cKO mice with abdominal UDT had an increase in serum follicle-stimulating hormone and luteinizing hormone and an absence of germ cells in the undescended testicle. *Wnt4*-cKO mice with inguinal UDT had normal hormonal profiles, and 50% of these mice had no sperm in the left epididymis. *Wnt4*-cKO mice had fertility defects and produced 52% fewer litters and 78% fewer pups than control mice. *Wnt4*-cKO testes demonstrated increased expression of estrogen receptor α and SOX9, upregulation of female gonadal genes, and a decrease in male gonadal genes in both CDT and UDT. Several *WNT4* variants were identified in boys with UDT. The presence of UDT and fertility defects in *Wnt4*-cKO mice highlights the crucial role of *WNT4* in testicular development.

KEY WORDS: Cryptorchidism, Infertility, WNT4, Gubernaculum, SOX9, Undescended testis

INTRODUCTION

Disorders of sex development are a major health issue. Cryptorchidism, or undescended testis (UDT), is one of the most common male congenital abnormalities, affecting 1-6% of full-term newborn males worldwide (Kolon et al., 2014; Virtanen and Toppari, 2008). The majority (82%) of patients with UDT have only one cryptorchid testis, which can be located in the abdomen (15%), the inguinal canal (25%) or the high scrotum (60%) (Kolon et al., 2014). In 5-10% of cases, the cryptorchid testes are either absent or atrophic as a result of early maldevelopment (Grady et al., 1998; Spires et al., 2000). Although the underlying mechanism driving UDT is rarely identified, overall fetal development is essential for

[1]Scott Department of Urology, Baylor College of Medicine, Houston, TX 77030, USA. [2]Center for Reproductive Medicine, Baylor College of Medicine, Houston, TX 77030, USA. [3]Department of Surgery, Nemours Children's Health, Orlando, FL 32827, USA. [4]Department of Molecular and Human Genetics, Baylor College of Medicine, Houston, TX 77030, USA. [5]Baylor Genetics Laboratories, Baylor College of Medicine, Houston, TX 77030, USA. [6]Department of Biochemistry and Molecular Biology, Baylor College of Medicine, Houston, TX 77030, USA.

*Author for correspondence (cj129804@bcm.edu)

C.J.J., 0000-0001-9203-6331

testicular descent, as premature or low-birth-weight boys are at an increased risk of UDT. Equally important is hormonal signaling, as suggested by the increased risk of UDT among boys born to mothers exposed to estrogen during pregnancy or boys with androgen insensitivity (Barthold et al., 2016; Komarowska et al., 2015). Surgical treatment (orchiopexy), which anchors the undescended testis to the scrotum, is performed in boys with UDT to preserve the testis for hormone and germ cell production and to reduce the likelihood of testicular cancer later in life (Feyles et al., 2014; Kollin et al., 2012; Lipshultz et al., 1976; Pike et al., 1986). Despite prompt surgical intervention during infancy, patients with surgically corrected UDT still manifest fertility issues, which may have a significant impact on their lives. In fact, UDT is the most common cause of nonobstructive azoospermia in men (Feyles et al., 2014; Hadziselimovic and Herzog, 2001b; Jarow et al., 1989; Kollin et al., 2012; Kolon et al., 2014). Interestingly, unilateral UDT can be a bilateral defect. Although the contralateral descended testis (CDT) in patients with unilateral UDT had previously been thought to have normal histology and fertility potential (Ritzén et al., 2007), 13% of men with treated unilateral UDT have been shown to be azoospermic (Hadziselimovic et al., 2011; Hadziselimovic and Herzog, 2001a; Verkauskas et al., 2019). Two different studies indicated that boys with unilateral UDT manifest bilateral testicular impairment (Barbotin et al., 2019; Verkauskas et al., 2019). A decrease in the number of spermatogonial stem cells is observed in both testes of boys with unilateral UDT. Furthermore, among boys with UDT, an absence of A-dark (Ad) spermatogonia (the reserve spermatogonia stem cells) was observed in 48% of cryptorchid testes and 21% of descended contralateral testes. These findings suggest that UDT results in abnormalities in both testes, including the CDT (Verkauskas et al., 2019). Interestingly, outcomes of testicular sperm extraction (TESE) in men with a history of unilateral versus bilateral UDT are similar (Barbotin et al., 2019). Given that current treatment strategies have not maximized future fertility potential in males with UDT, there is an urgent need to understand the mechanisms associated with infertility in this population.

During early development of the urogenital tract, the genital mesentery, which is composed of the cranial suspensory ligament and the caudal genital ligament, or gubernaculum, connects the testis to the abdominal wall (Zimmermann et al., 1999). Testicular descent occurs in two morphologically distinct phases that are under differential genetic control (Feng et al., 2009; Hutson et al., 2015). The transabdominal phase occurs prenatally in both humans (8-15 weeks gestation) and mice [embryonic days (E) 15.5-17.5]. During this phase, the cranial suspensory ligament regresses by the action of androgens and the gubernaculum is remodeled and enlarges as a result of the action of insulin-like hormone 3 (*Insl3*), a hormone secreted by Leydig cells. More specifically, the gubernaculum changes from a solid intra-abdominal pyramid to a protruding cone, which is lined by the peritoneum and has a central

cord attached to the caudal epididymis and testis. Both the regression of the cranial suspensory ligament and enlargement of the gubernaculum lead to the transabdominal testicular migration into the inguinal region. The inguinoscrotal phase occurs prenatally in humans (25-35 weeks gestation) and postnatally in mice (5-20 days old). This phase is characterized by the testosterone-mediated migration of the gubernaculum through the external ring and the final localization to the scrotum. Androgens regulate gubernacular migration via the genitofemoral nerve, which produces calcitonin gene-related peptide (Lie and Hutson, 2011). Despite their importance in testicular descent, only limited cases of UDT can be associated with defects in *Insl3* and androgen signaling (Ferlin et al., 2009, 2008; Suzuki et al., 2001; Wiener et al., 1998). Therefore, there must be additional signaling pathways that govern swelling and migration of the gubernaculum during testicular descent that remain to be elucidated.

WNT signaling is essential for gonadal development. *Wnt4* is initially expressed in somatic cells in the gonads of both sexes, but Wnt4 expression becomes ovary specific after sex determination at E12.5 (Jeays-Ward et al., 2004). Female mouse embryos that lack *Wnt4* develop testicular structures at birth (Ottolenghi et al., 2007; Vainio et al., 1999). By contrast, loss of *Wnt4* signaling in male embryos results in delayed testicular development (Jeays-Ward et al., 2004, 2003). As such, *Wnt4* has been shown to play a crucial role in the sex-specific patterning of the bipotential gonad for both sexes. Given its fine-tuned roles in different contexts, Wnt4 signaling must be tightly controlled for gonadal development.

We investigated the role of *Wnt4* in testicular descent by crossing retinoic acid receptor β2-*cre* mice with Wnt4-flox mice to generate a gubernaculum-specific conditional KO of *Wnt4* (*Wnt4*-cKO). We were able to identify WNT4 as an important signaling protein for testicular descent by showing that all *Wnt4*-cKO mice had significantly smaller left unilateral UDT. Although these mice had a CDT, the presence of fertility defects supports our hypothesis that unilateral UDT is a bilateral defect.

RESULTS
Targeted gubernacular deletion of *Wnt4* in mice results in unilateral UDT
WNT4 is a key regulator of sexual development (Jeays-Ward et al., 2004; Vainio et al., 1999). Mice with global KO of *Wnt4* die within 24 h after birth as a result of kidney abnormalities (Stark et al., 1994). WNT4 is highly expressed in the embryonic and adult ovary, and it is required for normal ovarian follicle development and function (Boyer et al., 2010; Hsieh et al., 2002). In the embryonic testes of mice, *Wnt4* is repressed by E12.5 by the FGF signaling pathway (Jameson et al., 2012). WNT4 it is highly expressed in the adult gubernaculum (Fig. 1A), suggesting its possible role in testicular descent, but it has a very low adult testicular expression level (Jorgez et al., 2021; Fig. 1B).

To study the role of *Wnt4* in testicular descent, a Cre-loxP approach, whereby *Wnt4*$^{fl/fl}$ mice (Kobayashi et al., 2011) were crossed to retinoic acid receptor β2 (*Rarb*) *cre* mice (Kobayashi et al., 2005), was implemented. This crossing generated gubernaculum-specific *Wnt4* conditional KO mice, herein called *Wnt4*-cKO. The *Rarb-cre* transgene is expressed in mesenchymal cells of the gubernacular bulb, epithelial cells of the gubernacular ligament, gubernacular striated muscle cells, the epididymis, the deferent duct, and Leydig cells of the testis in newborn mice (Kaftanovskaya et al., 2012). Crossing of *Rarb-cre* with the reporter line *Gt(ROSA)26Sor$^{tm14(CAG-tdTomato)Hze}$* revealed Cre expression indicated by mCherry antibody in both the adult gubernaculum

(Fig. 1C) and the interstitial cells of the testis (Fig. 1D). *Rarb-cre* mice have been used previously to study the role of *Rxfp2*, *Ctnnb1*, *Notch1*, *Ar* and *Wt1* genes in gubernacular development (Kaftanovskaya et al., 2011, 2012, 2013). All of these mouse models, with the exception of *Wt1-cKO*, have bilateral UDT.

Wild-type (WT) mice expressed WNT4 in the gubernaculum (Fig. S1A), but no *Wnt4*-cKO mice expressed WNT4 (Fig. S1D), suggesting a high efficiency of gubernaculum-specific recombination. Importantly, *Wnt4* deletion in the gubernaculum did not affect the expression of androgen receptor (AR) in the gubernaculum as WT mice gubernaculum (Fig. S1B) has similar AR expression pattern as the gubernaculum of *Wnt4*-cKO mice (Fig. S1E). To demonstrate the gubernaculum-specific recombination of Wnt4, the epithelium of the deferent duct of *Wnt4*-cKO mice was also stained, indicating specific WNT4 expression (Fig. S1G) as AR is not expressed in the epithelium of the deferent duct of *Wnt4*-cKO mice (Fig. S1H).

Wnt4-cKO mice show 100% penetrance of left unilateral UDT compared with WT mice (*n*=15; Fig. 2A,B, Table 1). The *Wnt4*-cKO left UDT was significantly smaller than the CDT (Fig. 2C,D), and the position of the left UDT varied from the inguinal canal to the abdomen (Table 1).

Mice with *Wnt4*-deficient gubernaculum have testicular and gubernacular abnormalities
In mice, the testicular descent from the abdominal cavity to the inguinal region occurs between E15.5 and E17.5, whereas the final descent into the scrotum takes place between 5 and 20 days postnatally (Feng et al., 2009; Hutson et al., 2015). WT mice testes on postnatal day 3 had similar morphology and distribution of Sertoli cells (SOX9-positive cells) and CCND1-positive spermatogonia (Fig. S2A-C) to age-matched *Wnt4*-cKO mice (Fig. S2D-F). Also, the histology of WT mice testes at postnatal day 14 (Fig. S2G-I) was similar to that of age-matched *Wnt4*-cKO mice (Fig. S2J-L). However, after puberty (3 weeks postnatal) some differences were observed in the left UDT. Compared with age-matched WT mice (Fig. S2M-O), *Wnt4*-cKO mice testes at postnatal day 21 had seminiferous tubules (STs) lacking layers of germ cells (Fig. S2P-R).

Testicular descent is dependent on the gubernaculum, and its migration into the scrotum determines the final position of the testis (Hutson and Hasthorpe, 2005). The left gubernaculum in the abdominal UDT was always thinner and longer than the right one (Fig. 2C). Further analysis of the gubernaculum using Masson's trichrome to highlight muscle fibers and collagen (Fig. 3A-E) indicated that the abdominal left UDT (Fig. 3E) had significantly less muscle and collagen content than the WT testis (Fig. 3A), the CDT (Fig. 3B) and the inguinal UDT (Fig. 3C,D). These data show that testicular descent and position are dependent on normal WNT4 signaling in the gubernaculum.

In sexually mature WT mice (after 6 weeks postnatal) normal ST (Fig. 3F) and sperm distribution in the epididymis (Fig. 3K) was observed. In sexually mature *Wnt4*-cKO mice with inguinal UDT, the CDT produced a normal sperm count with significantly (25%) reduced motility. Although most ST in the right CDT appeared normal, some STs had abnormal germ cell distribution with round cells in the lumen of the ST (Fig. 3G). Variability in the inguinal left UDT was observed in both weight (Fig. 2D) and histology (Fig. 3H,I), with some mice having some normal STs with a few abnormalities, including round cells in the lumen of the STs (Fig. 3H), whereas in other mice most of the STs exhibited maturation arrest (MA). MA is defined as an interruption of
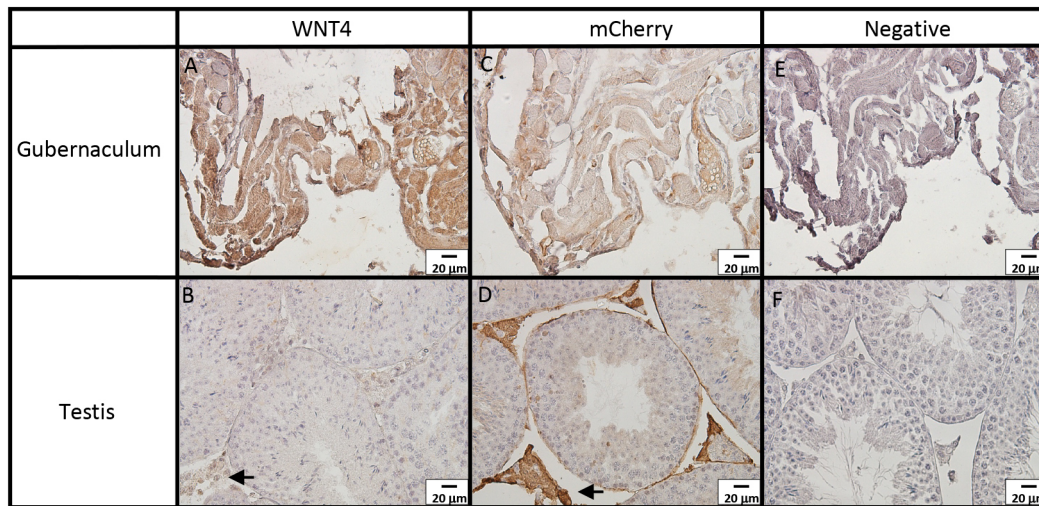
Fig. 1. WNT4 and retinoic acid receptor β2 (Rarb) expression in the testis and gubernaculum. *Rarb-cre* mice were crossed with the reporter line *Gt(ROSA)26Sor*^{tm14(CAG-tdTomato)Hze} to determine *Rarb-cre* expression in adult tissues. Gubernaculum and testis of four hemizygous mice were sectioned (5 µm) and stained with WNT4 and mCherry antibodies. (A) WNT4 is highly expressed in the adult gubernaculum. (B) WNT4 has low adult testicular expression level with a low expression in the interstitial cells (black arrow). (C,D) mCherry antibody was used to detect the tdTomato reporter that indicated *Rarb* expression. mCherry was detected in the adult gubernaculum (C) and detected at high levels in the interstitial cells of the testis (black arrow). (E) Gubernaculum negative control. (F) Testis negative control (omission of primary antibody).

spermatogenesis before the final stage without Sertoli or Leydig cell impairment (Fig. 3I). The epididymides from the mice with MA testes showed round germ cells in the lumen (Fig. 3N). The epididymides from the CDT did not differ from those of WT mice (Fig. 3K,L). Overall, the sperm parameters of the inguinal left UDT were significantly abnormal with a 74% decrease in sperm count and a 97% decrease in sperm motility (Table 1).

In adult *Wnt4*-cKO mice with left abdominal UDT, both the left testis and epididymis were significantly smaller. These mice also exhibited a 'Sertoli cell only' (SCO) phenotype, defined as Sertoli cells lining the inside of the seminiferous tubules without germ cells (Table 1, Fig. 3J). The epididymides from the mice with SCO testes

showed empty tubules and a few round germ cells in the lumen (Fig. 3O). Although the right CDT was of normal size and produced a normal amount of sperm, the motility of these sperm was significantly reduced.

UDT is associated with primary testicular dysfunction leading to a high gonadotropin drive, elevated levels of follicle-stimulating hormone (FSH) and luteinizing hormone (LH), and normal levels of testosterone, especially in boys with intra-abdominal UDT (Suomi et al., 2006). Hormonal profiles of *Wnt4*-cKO males with inguinal left UDT did not differ from those of WT males (Fig. 4). However, male *Wnt4*-cKO mice with abdominal left UDT had significantly elevated levels of circulating LH and FSH compared with those of
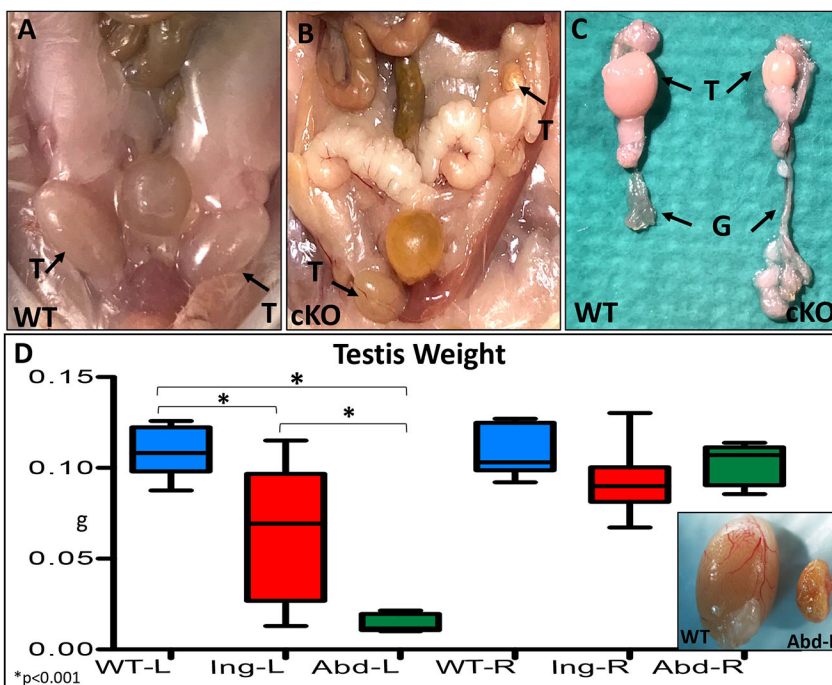

Fig. 2. *Wnt4*-cKO mice have left UDT. (A,B) Images indicating the testicular position in the abdominal cavity of WT mice with normal testicular descent into the scrotum (A) and *Wnt4*-cKO mice with right testis in the scrotum and left testis high in the abdominal cavity (B). (C) Left abdominal UDT in *Wnt4*-cKO is smaller with a longer gubernaculum compared with WT testis. (D) Comparison of testicular weight in WT (blue), *Wnt4*-cKO with inguinal UDT (red) and *Wnt4*-cKO with abdominal UDT (green). *n*=15; **P*<0.01 (one-way ANOVA). Box whiskers indicate minimum to maximum, middle line indicates mean, and the error bars indicate s.e.m. Abd, abdominal; G, gubernaculum; Ing, inguinal; L, left; R, right; T, testis.

Table 1. Sexual organ characteristics and sperm profile of *Wnt4*-cKO mice

	WT *n*=6	KO-Inguinal *n*=9	KO-Abdominal *n*=6
Left testis (mg)	108.8±13.8	**63.0±36.9***	**14.1±4.8***
Right testis (mg)	111.0±14.7	92.36±18.5	102.7±11.2
Left epididymis (mg)	52.6±9.6	44.9±15.2	**26.1±11.4***
Right epididymis (mg)	52.1±10.0	48.1±11.0	46.1±17.9
Left CM (mg)	19.6±10.2	20.3±18.3	20.9±18.5
Right CM (mg)	18.4±3.4	15.6±7.9	15.0±1.3
Left sperm count (10^6/ml)	14.7±2.2	**3.9±6.7***	**0***
Right sperm count (10^6/ml)	16.5±1.8	16.0±6.0	15.8±6.2
Left sperm motility (%)	37.9±5.6	**1.2±2.0***	**0***
Right sperm motility (%)	40.4±8.5	**30.2±10.0***	**26.0±6.8***

CM, cremaster muscle. Values in bold indicate significance (*$P<0.01$ compared with WT mice). Data are presented as mean±s.e.m., and were analyzed using one-way ANOVA with Bonferroni correction.

male WT mice and *Wnt4*-cKO mice with inguinal left UDT (Fig. 4A,B). The levels of testosterone did not significantly differ between groups (Fig. 4C). The hormonal profiles of *Wnt4*-cKO mice with abdominal UDT mimic findings described in humans with abdominal UDT (Suomi et al., 2006).

Cryptorchidism in *Wnt4*-cKO mice alters their fertility potential

We assessed fertility of mutant mice by naturally mating 6-week-old *Wnt4*-cKO males with WT females (Fig. 5). At the time of mating, the position of testes in both groups was unknown. After 6 months of mating, the male mice were sacrificed, and their testicular position was evaluated. Each of the eight WT mice was considered fertile because they produced six litters with an average number of pups per litter of 8.2±0.7 for a total of 48 litters (Fig. 5A,B). Of the eight *Wnt4*-cKO males, three had inguinal left UDT. One of these three mice with UDT produced the same number of litters as the WT mice (*n*=6), but had 50% fewer pups per litter (4.1±0.7 versus 8.2 ±0.7; *P*<0.01; average±s.e.m. analyzed using one-way ANOVA). The other two *Wnt4*-cKO with inguinal left UDT produced two and three litters, respectively, and had overall 50% fewer pups than WT mice, indicating that *Wnt4*-cKO males with inguinal left UDT were subfertile. Of the five *Wnt4*-cKO males with abdominal left UDT, one was infertile, and the remaining four had severe fertility defects with an average of 3.5±1.2 pups per litter (57% fewer than WT; *P*<0.01; average±s.e.m. analyzed using one-way ANOVA). At the end of the mating period, *Wnt4*-cKO mice produced 50% fewer litters, with the WT mice producing 48 litters and the *Wnt4*-cKO males producing 24 litters (Fig. 5B). In addition, *Wnt4*-cKO mice produced 76% fewer pups than WT mice (395 versus 93) (Fig. 5C).

Wnt4-cKO mice testis have disrupted testicular cellularity

To understand the cause of reduced fertility in *Wnt4*-cKO mice, we performed immunohistochemistry in testicular sections (Figs 6 and 7). Although immunohistochemistry does not allow for quantification of protein levels, it was an important tool to determine whether certain cell populations were affected. Immunohistochemistry was especially important given that *Wnt4*-cKO left UDT has a wide range of histological phenotypes, such as MA and SCO. Protein quantification of testes with these phenotypes can be biased because of the lack of a specific cell type.

The presence of 3β-hydroxysteroid dehydrogenase (3β-HSD), a Leydig cell protein involved in the biosynthesis of testosterone, was examined because its expression has been shown to be reduced in rodent abdominal testes (Niewenhuis, 1980). 3β-HSD was expressed in both WT and *Wnt4*-cKO (Fig. 6A-D). Immunohistochemistry of promyelocytic leukemia zinc finger protein (PLZF; also known as ZBTB16), a marker of undifferentiated spermatogonia, indicated the presence of PLZF-positive cells in WT testes, *Wnt4*-cKO CDT and *Wnt4*-cKO UDT (Fig. 6E-H). These results correlate with the levels of PLZF-positive cells in *Rxfp2* KO cryptorchid testes at 3 months of age (Ferguson et al., 2013). The proliferative activity of spermatogonia is decreased in cryptorchid testes of male children (Markewitz et al., 1970). Expression of the cell proliferation markers CCND1 and KI67 (MKI6) positively correlates with spermatogenesis because both are expressed in proliferating spermatogonia. However, KI67 is also expressed in differentiating spermatogonia (Beumer et al., 2000; Zhao et al., 2018). CCND1-positive cells were decreased only in *Wnt4*-cKO abdominal UDT because these abdominal testes lack most germ cells (Fig. 6I-L). Interestingly, KI67-positive cells were decreased in all *Wnt4*-cKO testes independent of their position (Fig. 6M-P, Fig. S3), mimicking the low levels of KI67 seen in the testes of oligozoospermic men (Steger et al., 1998) and non-mouse models of unilateral UDT (Moon et al., 2014).

Leydig cells are the major source of testicular estrogen synthesis and action (Banerjee et al., 2012). Estrogen receptor alpha (ERα; ESR1) is expressed strongly in Leydig cells of cryptorchid testes, but weakly in those of control rodents (Mizuno et al., 2011). In *Wnt4*-cKO mice, ERα was highly expressed in Leydig cells of inguinal and abdominal left UDT as well as the right CDT, but its expression was very low in WT testis (Fig. 7A-E). SOX9 is a marker of Sertoli cells that has been associated with improved fertility prognosis in cryptorchid boys because boys with Ad spermatogonia at surgery had a higher number of SOX9 Sertoli cells compared with boys without Ad spermatogonia (Hildorf et al., 2019). SOX9-positive cells were present in WT testes as well as *Wnt4*-cKO CDT and UDT (Fig. 7F-J). Interestingly, the testes of *Wnt4*-cKO with inguinal UDT had a higher number of SOX9-positive cells per ST cross-section compared with the testes of WT mice (Fig. 7K).

Gonad development is disrupted in *Wnt4*-cKO mice testis

To understand the effect of *Wnt4*-induced cryptorchidism on testicular gene expression, quantitative PCR (qPCR) was performed for 27 genes (Fig. 8A) associated with the cell cycle (orange), the WNT pathway (yellow), male gonad sex determination and function (blue) and female gonad sex determination and function (pink). Relative gene quantification compared the WT testes with UDT and CDT of *Wnt4*-cKO mice with inguinal and abdominal UDT. The abdominal left testes showed the most differential gene expression profile compared with WT, CDT and inguinal UDT, likely because of the absence of germ cells (Fig. 8A; *P*<0.005; analyzed using one-way ANOVA). Some genes that are important in male sexual development, such as *Cyp19a1*, *Gdnf*, *Dmrt1*, *Dhh* and *Lgr8* were downregulated in *Wnt4*-cKO CDT and UDT. By contrast, *Wnt4*-cKO testes revealed an upregulation of genes essential for female gonadal development and function, such as *Rspo1*, *Wnt4* and *Foxl2* in both CDT and UDT. To corroborate the gene expression data, we performed a western blot of BMP4 in the testes of WT and *Wnt4*-cKO mice (Fig. 8B). Variations were observed in the levels of BMP4; some *Wnt4*-cKO mice showing no increase whereas others had a higher expression of protein, with an average twofold increase in *Wnt4*-cKO mice (Fig. 8B). The expression of WNT4 in the testes of
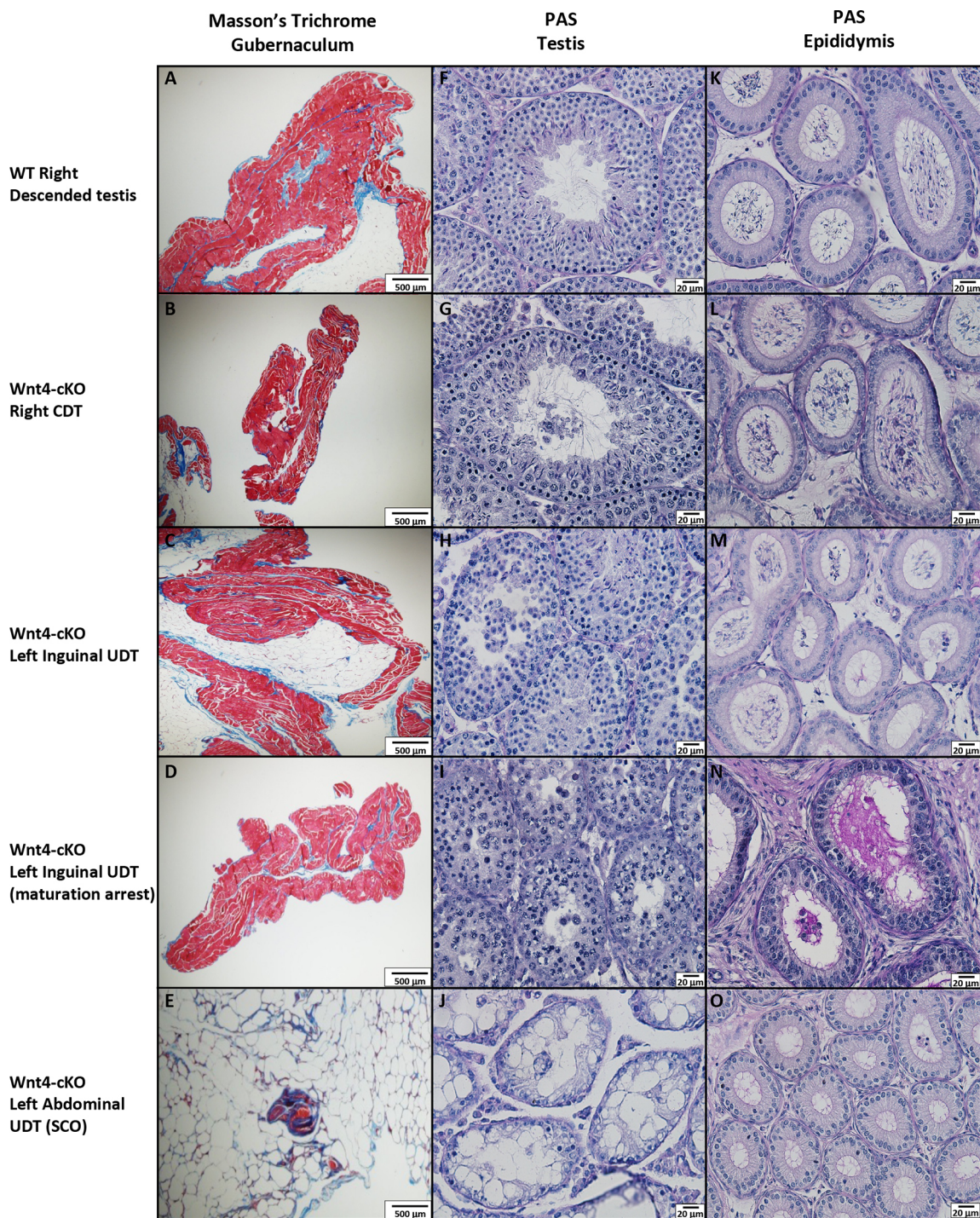
DEVELOPMENT

4

Fig. 3. *Wnt4*-cKO have gubernacular, testicular and epididymal abnormalities. (A-E) Masson's trichrome staining of mouse gubernaculum from different mice indicating muscle (red) and collagen (blue) content. (F-J) Testicular comparison using PAS staining of WT and *Wnt4*-cKO mice with testes of different positions. (F) WT mice displaying normal ST morphology and distribution. (G) Right-CDT displaying some abnormalities, including the presence of round cells in the lumen of STs. (H) Inguinal-UDT testes of *Wnt4*-cKO mice displaying some abnormalities, including the presence of round cells in the lumen of STs. (I) Inguinal-UDT testes of *Wnt4*-cKO mice displaying an MA phenotype. (J) Abdominal-UDT testes of *Wnt4*-cKO mice displaying an SCO phenotype. (K-O) Epididymal comparison using PAS staining of WT and *Wnt4*-cKO mice. (K) WT mice displaying abundant sperm in the epididymis. (L,M) *Wnt4*-cKO R-CDT mice (L) and *Wnt4*-cKO inguinal L-UDT mice (M) displaying abundant sperm in the epididymis with some isolated round cells. (N,O) *Wnt4*-cKO inguinal L-UDT mice (N) and *Wnt4*-cKO abdominal L-UDT mice (O) displaying a few round cells only.

WT and *Wnt4*-cKO mice was determined (Fig. S4). WNT4 in WT mice was expressed only in the interstitial cells (Fig. S4A,B). In *Wnt4*-cKO mice, WNT4 was expressed in both the interstitial cells and inside the ST (Fig. S4C-H), which could explain the upregulation

observed in *Wnt4* mRNA levels (Fig. 8A). The presence of WNT4 in interstitial cells of *Wnt4*-cKO testes suggests that *Rarb-cre* recombination is not highly efficient in this cell population. Detailed graphs showing fold difference and fold and ΔC*t*
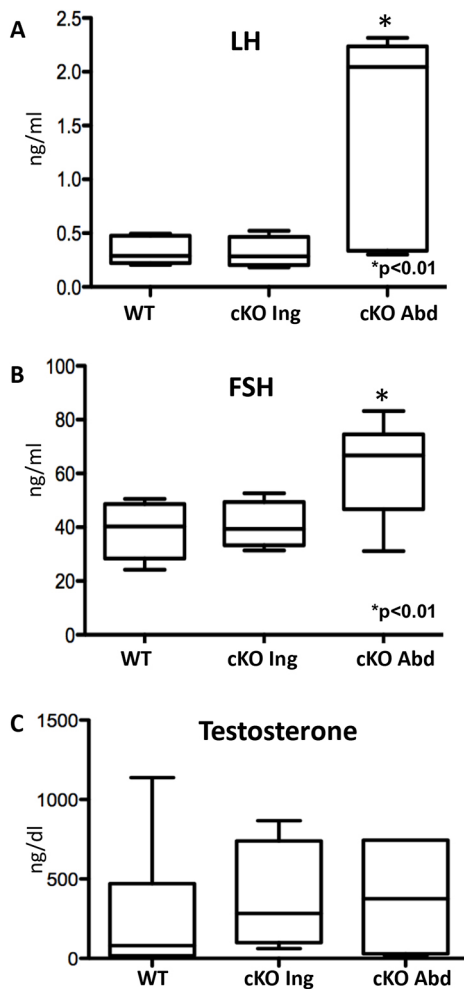
Fig. 4. *Wnt4*-cKO mice with abdominal UDT have elevated levels of FSH and LH. (A-C) Comparison of levels of serum testosterone (A), LH (B) and FSH (C) among five mice from each of the following groups: WT, *Wnt4*-cKO with inguinal UDT (cKO-Ing) and *Wnt4*-cKO with abdominal UDT (cKO-Abd). *$P<0.01$ (one-way ANOVA). Box whiskers indicate minimum to maximum, middle line indicates mean, and the error bars indicate s.e.m.

Fig. 5. *Wnt4*-cKO mice show fertility defects. (A) Graph showing fertility of male mice after 6 months of mating with WT females. All eight WT males produced one litter per month and were considered fertile (blue bar). Of the eight *Wnt4*-cKO males, three had left inguinal UDT (red) and five had abdominal UDT (green). All the *Wnt4*-cKO with inguinal UDT were subfertile. Of the *Wnt4*-cKO with abdominal UDT, one was infertile and the other four were subfertile. (B) Total number of litters produced per mouse group over a period of 6 months. Each of the eight WT male mice produced six litters for a total of 48 litters in a 6-month period (blue line). The three *Wnt4*-cKO with inguinal UDT produced a total of 11 litters in a 6-month period (red line), similar to the five *Wnt4*-cKO with abdominal UDT that produced a total of 13 litters in a 6-month period (green line). All *Wnt4*-cKO (yellow line) produced a total of 24 litters, which was significantly different ($P<0.01$; one-way ANOVA) from WT mice. (C) Total number of pups produced per mouse group over a period of 6 months. The eight WT male mice produced a total of 395 pups in a 6-month period (blue line). The three *Wnt4*-cKO with inguinal UDT produced a total of 47 pups in a 6-month period (red line), similar to the five *Wnt4*-cKO with abdominal UDT that produced a total of 46 pups in a 6-month period (green line). All *Wnt4*-cKO (yellow line) produced a total of 93 pups, which was significantly different ($P<0.01$; one-way ANOVA) from WT mice.

differences in individual mice of genes significantly differentially expressed in *Wnt4*-cKO mice versus WT mice are given in Figs S5 and S6.

WNT4 variants identified in patients with UDT and genitourinary (GU) tract defects

We investigated variants in *WNT4* among 17,000 individuals undergoing clinical exome sequencing (ES) (Chen et al., 2020; Yang et al., 2014). The main phenotypic presentation of the individuals in this group was nervous system dysfunction, with only 398 (2.3%) having any indication of UDT. Of the 142 individuals that had single nucleotide variants (SNVs) in *WNT4*, six of them had UDT (4.2%). Five distinct SNV in *WNT4* were identified in individuals with UDT (Table 2). Q167H was identified in only one individual in a homozygous state. Q167H has not been reported in the Single Nucleotide Polymorphism Database (dbSNP), Genome Aggregation Database (gnomAD) or Trans-Omics for Precision Medicine (TOPMed) database, suggesting that it is extremely rare in the general population. Y80H, R258C and Q282R were each identified in a heterozygous state in a different boy with UDT, and
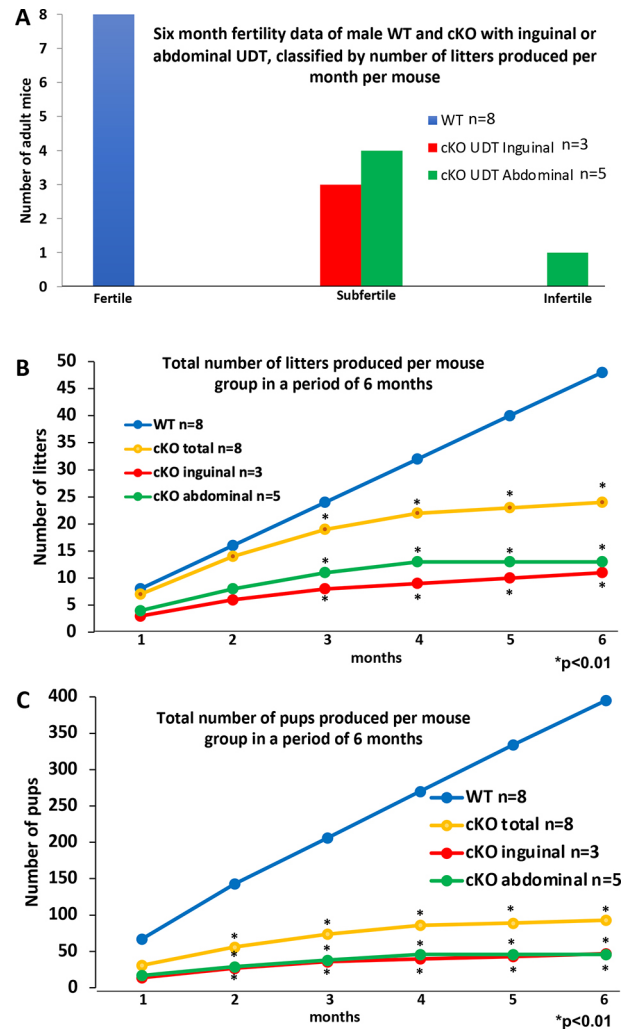
heterozygous P264Q was identified in two boys with UDT. These last four single nucleotide polymorphisms were identified in a few additional individuals in the Baylor Genetics clinical ES database as well as the TOPMed and gnomAD databases. The boy carrying Y80H and the boy carrying P264Q had kidney abnormalities, which are common defects associated with *WNT4* defects (Kiewisz et al., 2019; Vivante et al., 2013).
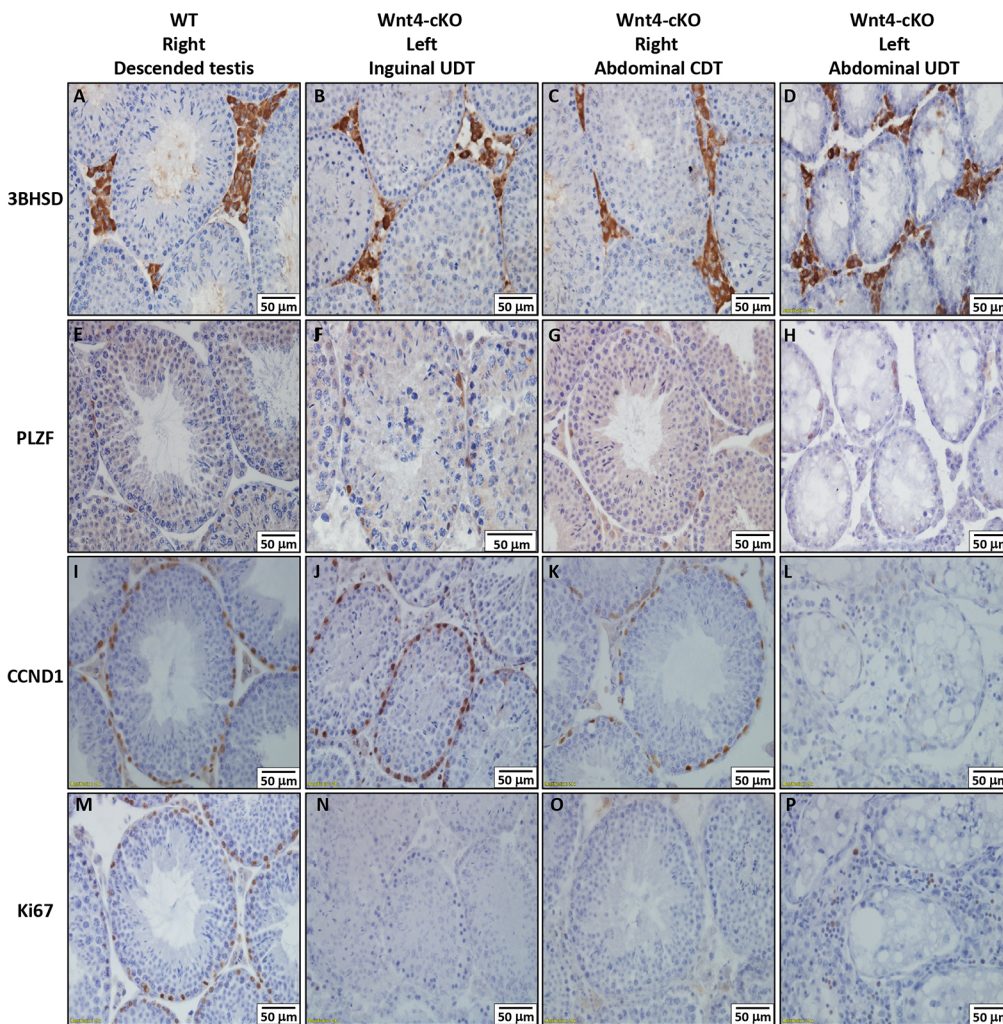
DEVELOPMENT

Fig. 6. Characterization of *Wnt4*-cKO CDT and UDT in different testicular cell populations. Testes of WT, *Wnt4*-cKO left inguinal UDT, *Wnt4*-cKO abdominal right CDT and *Wnt4*-cKO left abdominal UDT were stained with different testicular cell markers. (A-D) Leydig cells showed 3β-HSD expression in all testes analyzed. (E-L) The spermatogonial markers PLZF (E-H) and CCND1 (I-L) were expressed in all testes analyzed including the abdominal UDT, in which most of the STs exhibited an SCO phenotype. (M-P) The spermatogonial marker KI67 was highly expressed in WT spermatogonia, but not in *Wnt4*-cKO spermatogonia independent of the testis position.

Pathogenic mutations in *WNT4* have been identified in other pathologies (Biason-Lauber et al., 2007, 2004; Mandel et al., 2008; Philibert et al., 2011). To investigate whether these *WNT4* variants are damaging, we sought to perform structural analyses of WNT4 protein. The homology model of WNT4 was built on the SWISS-MODEL server using chain B of the crystal structure of the human WNT3 with the complex mouse frizzled 8 Cys-rich domain (CRD) as the template. Sequence alignment of WNT4 and WNT3 shows that they share 51.46% sequence identity (Fig. 9A). WNT4 is a hydrophobic, glycosylated and acetylated signaling protein (Fig. 9A). The architecture of the WNT4 homology model is the same as that of hWNT3 or xWNT8, with an N-terminal signal peptide (SP) that corresponds to the first 22 amino acids, followed by the N-terminal domain (NTD), the linker region and the elongated C-terminal domain (CTD) (Fig. 9B).

Structural modeling of the Y80H variant shows that substituting the aromatic tyrosine with a basic histidine residue at position 80 alters the surface charge within the region of the NTD (Fig. 9C). The residue Q167 in WT WNT4 is adjacent to two positively charged residues, R175 and R195. The Q167H variant may also change the surface charge or affect the protein stability of the mutant (Fig. 9D). Moreover, residues R258 and P264 are located within the linker region, which has the greatest sequence variability compared with other species. It was thought that the linker region contains the binding site for WNT-specific co-receptors, such as the low-density

lipoprotein receptor (LDLR)-related 6 (LRP6). Variants R258C and P264Q may lead to loss of binding or decreased affinity towards the co-receptors of WNT4, thereby affecting testicular development (Fig. 9E). Residue Q282 resides in a flexible loop in the CTD. Substitution of Q282 with arginine may not affect the structure of the loop. Therefore, the prediction software suggests that the Q282R variant could be a benign polymorphism or non-pathogenic (Fig. 9F, Table 2). Future structural and biochemical studies are needed to clarify the effects of these *WNT4* variants on protein stability, interaction with other cellular receptors, and the roles of these receptors during development.

DISCUSSION

This study addresses a long-standing and important clinical question – why do boys with unilateral UDT have an increased risk of infertility despite early surgical correction? The majority of studies evaluating the etiology of UDT have thus far focused on the second phase of testicular descent and the role of androgen action during GU development (Docampo and Hadziselimovic, 2015). Although androgen signaling is necessary, it is not solely sufficient for testicular descent. Cryptorchidism occurs most often in males who have normal androgen receptor function (Wiener et al., 1998). We developed a unique model of unilateral UDT in mice that indicates that WNT4 signaling plays an important role in testicular descent and fertility. In addition, we identified several variants in
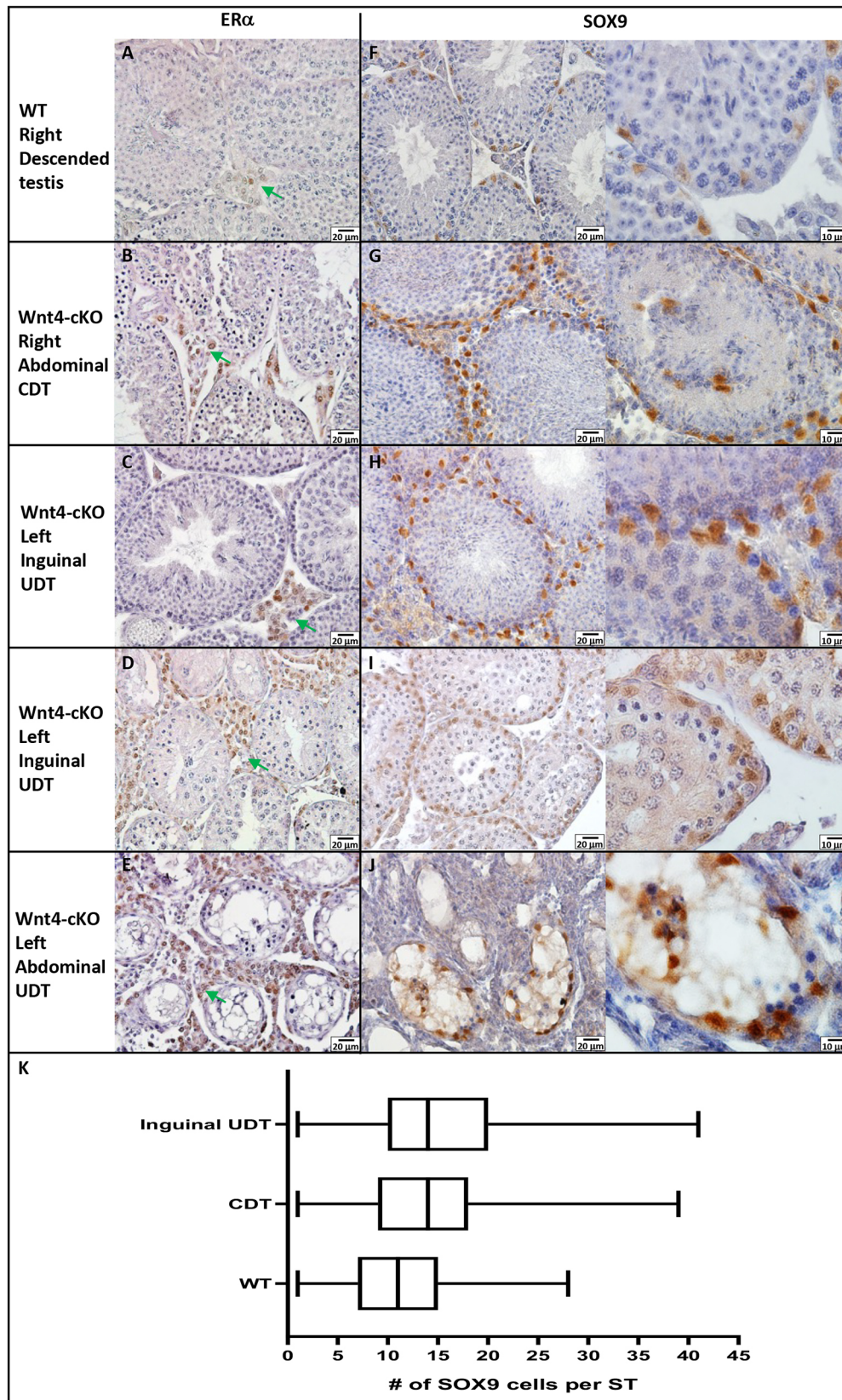
Fig. 7. *Wnt4*-cKO mice have increased ERα and SOX9. Testes of WT, *Wnt4*-cKO abdominal right CDT, left inguinal UDT (showing normal-appearing ST or MA) and *Wnt4*-cKO left abdominal UDT were stained for ERα and SOX9. (A-E) Leydig cells showed ERα expression (green arrow) in all testes analyzed, but *Wnt4*-cKO testes had more ERα-expressing cells than did WT testes. (F-J) Expression of the Sertoli cell marker SOX9 at low and high magnification indicates an increase in the number of SOX9-positive cells in *Wnt4*-cKO testes independent of the position. (K) Quantification of the number of SOX9-positive cells in WT testes (10.4±4.5) and in *Wnt4*-cKO inguinal CDT (15.4±7.5) and UDT (21.2±7.5) indicates a significant increase of SOX9-positive cells in *Wnt4*-cKO mice compared with WT mice (*P*<0.001; one-way ANOVA).

WNT4 in boys with cryptorchidism that could potentially cause or contribute to their condition.

One unique finding of the *Wnt4*-cKO model was that 100% of these mice presented with unilateral left UDT. Most mouse models of cryptorchidism show bilateral UDT with the exception of *Wt1-Rarb-cre*-cKO mice, which have left-sided cryptorchidism in 39% of males and no fertility defects (Kaftanovskaya et al., 2011, 2012, 2013). In boys with normally descended testes, the right testis
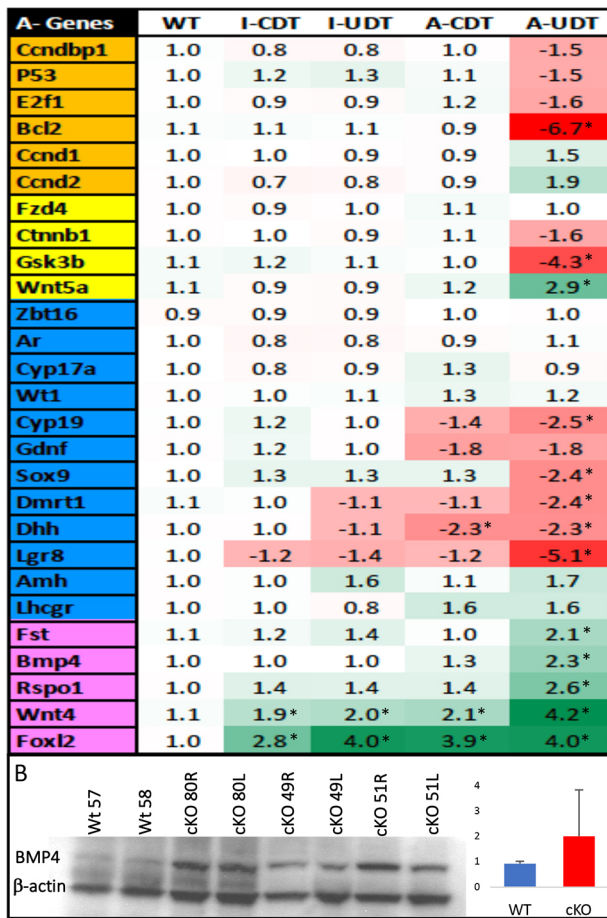
A- Genes	WT	I-CDT	I-UDT	A-CDT	A-UDT
Ccndbp1	1.0	0.8	0.8	1.0	-1.5
P53	1.0	1.2	1.3	1.1	-1.5
E2f1	1.0	0.9	0.9	1.2	-1.6
Bcl2	1.1	1.1	1.1	0.9	-6.7*
Ccnd1	1.0	1.0	0.9	0.9	1.5
Ccnd2	1.0	0.7	0.8	0.9	1.9
Fzd4	1.0	0.9	1.0	1.1	1.0
Ctnnb1	1.0	1.0	0.9	1.1	-1.6
Gsk3b	1.1	1.2	1.1	1.0	-4.3*
Wnt5a	1.1	0.9	0.9	1.2	2.9*
Zbt16	0.9	0.9	0.9	1.0	1.0
Ar	1.0	0.8	0.8	0.9	1.1
Cyp17a	1.0	0.8	0.9	1.3	0.9
Wt1	1.0	1.0	1.1	1.3	1.2
Cyp19	1.0	1.2	1.0	-1.4	-2.5*
Gdnf	1.0	1.2	1.0	-1.8	-1.8
Sox9	1.0	1.3	1.3	1.3	-2.4*
Dmrt1	1.1	1.0	-1.1	-1.1	-2.4*
Dhh	1.0	1.0	-1.1	-2.3*	-2.3*
Lgr8	1.0	-1.2	-1.4	-1.2	-5.1*
Amh	1.0	1.0	1.6	1.1	1.7
Lhcgr	1.0	1.0	0.8	1.6	1.6
Fst	1.1	1.2	1.4	1.0	2.1*
Bmp4	1.0	1.0	1.0	1.3	2.3*
Rspo1	1.0	1.4	1.4	1.4	2.6*
Wnt4	1.1	1.9*	2.0*	2.1*	4.2*
Foxl2	1.0	2.8*	4.0*	3.9*	4.0*

Fig. 8. Altered gene expression profile in *Wnt4-cKO* mouse testes.
(A) qPCR analysis of 27 selected genes. Colors indicate gene categories: cell cycle (orange), WNT pathway (yellow), male gonad sex determination and function (blue) and female gonad sex determination and function (pink). Relative gene quantification compared with WT testes (normalized to 1) is indicated for both testes of mice with inguinal UDT and abdominal UDT as well as the corresponding CDT. The numerical quantification is indicated. Genes that were downregulated are lower than 1 and indicated by variants of red color depending on the degree of downregulation. Genes that were upregulated are higher than 1 and indicated by variants of green color depending on the degree of upregulation. Statistical analyses were conducted using the REST Software from QIAGEN to determine significance (*P<0.005). (B) BMP4 western blots normalized to β-actin and quantified using ImageJ of WT left testis and both left and right testis of Wnt4-cKO with inguinal UDT. Graphs show western blot band intensities. Data are average±s.d.

embryogenesis by complex signaling mechanisms, including the WNT signaling pathway (Minegishi et al., 2017; Nakaya et al., 2005; Walentek et al., 2013). Disruption of the embryo's bilateral symmetry can result in a pathologic molecular left-right bias in the mesoderm, causing congenital defects (Desgrange et al., 2018). The mechanism by which laterality in testicular descent is generated is not well understood. However, a previous study in *Drosophila* showed that *Wnt4* plays an important role in governing left-right morphogenesis, particularly in the midgut (Kuroda et al., 2012). Some studies point to regulation of this left-right bias by AR and INSL3 in gubernacular development (Kaftanovskaya et al., 2011, 2012). The exact molecular mechanisms controlling differential gubernacular development remain unknown. Although WNT4 is expressed in both the left and right gubernaculum, it is possible that the left-biased role of WNT4 in testicular descent could be dictated by its regulation of a driver of left-right patterning, such as *Pitx2*. *Pitx2* potentiates asymmetric regulation of WNT signaling (Hendee et al., 2018; Welsh et al., 2013). Further studies are required to reveal the regulators of WNT4 in the gubernaculum and how WNT4 governs gubernacular development, testicular position and testicular symmetry.

Ten percent of infertile men from the general population have a history of UDT and orchiopexy (Chung and Brock, 2011). The incidence of azoospermia is 13% in unilateral UDT and 33% in bilateral UDT, independent of surgical correction (Chung and Brock, 2011; Hadziselimovic et al., 2011; Hadziselimovic and Herzog, 2001b). Interestingly, alterations in the number of spermatogonia are observed in both testes in boys with unilateral UDT (Verkauskas et al., 2019). Infertility in patients with unilateral and bilateral UDT is two and six times more common, respectively, than in the general population (Lee et al., 1996, 1997). UDT represents a major health problem and is a perplexing issue because boys with unilateral UDT theoretically should have a normal contralateral testis that produces sperm capable of successful oocyte fertilization. As described above, we developed a unique mouse model with 100% penetrance of unilateral UDT and fertility defects. This model has allowed us to improve our understanding of the difference in testicular function between UDT and normal-appearing CDT. In other models that present mainly with inguinal unilateral UDT, particularly *Wt1*-cKO, males are fertile, thus suggesting that the CDT compensates for the poorly functioning UDT or that there is a low penetrance of the phenotype (Kaftanovskaya et al., 2013). However, we showed in our model that the proliferative spermatogonia marker KI67 was significantly decreased in *Wnt4*-cKO CDT to levels similar to the low levels of KI67 observed in the testes of oligozoospermic men (Steger et al., 1998) and non-mouse models of unilateral UDT (Moon et al., 2014).

Increased expression of ERα in Leydig cells of cryptorchid testes is associated with an androgen-estrogen imbalance that leads to deterioration of spermatogenesis in UDT (Mizuno et al., 2011). In this study, an increase in ERα in Leydig cells was observed in both UDT and CDT, indicating that the androgen-estrogen imbalance affects both testes. It is unclear whether the defect in ERα expression is a direct consequence of the abnormal testicular descent or an effect of deficient WNT4 signaling in Leydig cells. WNT4 is highly expressed in Leydig cells in prepubertal testes of mice and continues to be expressed in adult testes (Jorgez et al., 2021). One caveat of this model is that Rarb-Cre and WNT4 are expressed in Leydig cells of the testis, and the fertility defect in *Wnt4*-cKO could be due to lack of WNT4 in Leydig cells. We previously reported that conditional deletion of *Wnt4* in the germ

is typically larger (Vaganée et al., 2018) and appears to complete descent first (Favorito and Sampaio, 2014). This left-right asymmetry is relatively common in certain vertebrate organs, and developmental abnormalities tend to occur with a left bias. For example, multiple congenital kidney anomalies (multicystic dysplastic kidney, renal agenesis/aplasia, renal ectopia, pelviureteric junction obstruction, and nonobstructive non-refluxing megaureter) occur significantly more often on the left side (Schreuder, 2011; Schreuder et al., 2009; Simonetti and Mohaupt, 2012). It has been shown in animal models that some anomalies, such as hydronephrosis, also have a left-sided bias (Matsuyama et al., 2013). The mechanisms leading to these alterations remain unknown, but may involve differential gene expression. Organ asymmetries are established during

Table 2. Variants in *WNT4* in boys with GU defects

WNT4 variant	Y80H	Q167H	R258C	P264Q	Q282R
Phenotype	UDT or bilateral hydronephrosis	UDT	UDT	UDT and hypospadias or right hydroureter	UDT and hypospadias
Number of boys	2	1	2	4	4
Number of affected boys	2 (1 UDT)	1	1	3 (2 UDT)	1
Location	Exon 2	Exon 4	Exon 5	Exon 5	Exon 5
Nucleotide*	c.238T>C	c.501G>C	c.772C>T	c.791C>A	c.845A>G
Zygosity	Heterozygous	Homozygous	Heterozygous	Heterozygous	Heterozygous
Polyphen2	Benign	Benign	Damaging	Damaging	Benign
MutationTaster	Disease causing	Disease causing	Disease causing	Disease causing	Polymorphism
SIFT	Damaging	Damaging	Damaging	Tolerated	Tolerated
dbSNP	rs201024257	Not reported	rs953737200	rs773876465	rs868186380
TOPMed	30/125,568	0	2/125,568	2/125,568	2/125,568
gnomAD	39/251,284	0	1/251,276	0	1/31,406

*According to NM_030761.4 transcript.
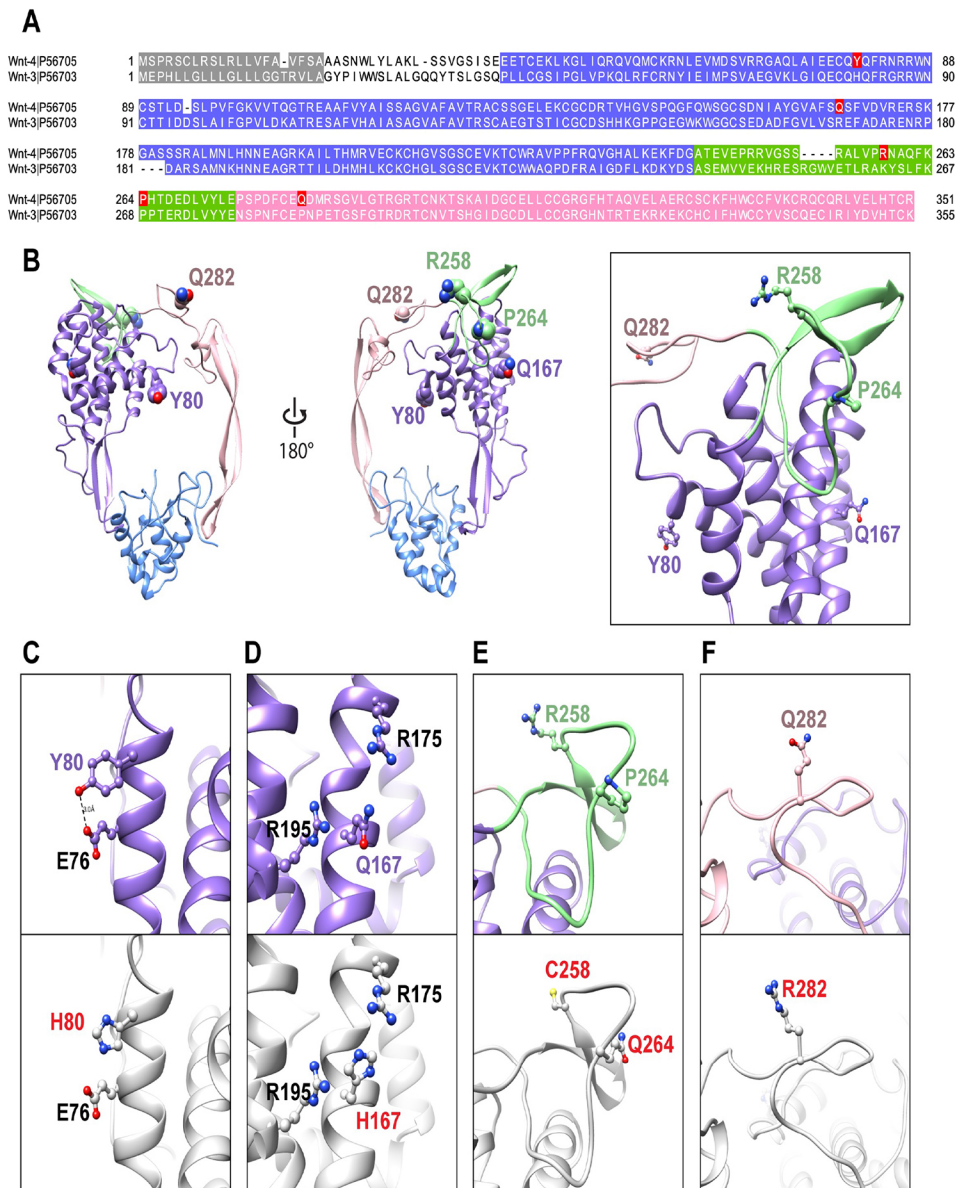
Fig. 9. Structural mapping of WNT4 variants in boys with GU defects.
(A) Sequence alignment of human WNT4 and WNT3 using Jalview. The sequences of the signal peptide, the WNT N-terminal domain (NTD), the linker region, and the elongated C-terminal domain (CTD) are highlighted in gray, purple, green and pink, respectively. The residues that are altered in boys with GU defects are labeled in red. The UniProtKB accession numbers are shown to the left of the sequences. (B) The homology model of WNT4 was superimposed onto the crystal structure of the WNT signaling complex (PDB ID: 6AHY), which consists of human WNT3 and mouse frizzled 8 Cys-rich domain (CRD). For clarity, the structure of WNT3 is not shown, and the Frizzled-8 CRD is shown in blue ribbon representation. Each domain of WNT4 is color coded as in A. The mutated residues of WNT4 are shown as spheres. The inset on the right shows the close-up view of residues affected by variants shown in ball-and-stick models. The atoms are colored with oxygen in red, nitrogen in blue and sulfur in yellow. (C-F) Close-up views of mutations (Y80H, Q167H, R258C, P264Q and Q282R) in WNT4. The WT residues are colored as in A, and the mutant models are shown in gray.

cells of male mice (using *Stra8*[cre/+] reporter mice) does not have a significant effect on fertility (Jorgez et al., 2021). There is no report of mice deficient in *Wnt4* in Leydig cells. However, WNT4 has an important role in steroidogenesis. This is evident in Leydig cell lines, in which induction of WNT4 leads to a significant reduction in 3β-HSD activity. Furthermore, *WNT4* transgenic male mice showed a dramatic reduction in steroidogenic acute regulatory protein levels as well as serum and testicular androgen levels (Jordan et al., 2003). Although Leydig cells are essential for the lifelong support of spermatogenesis, *Wnt4*-cKO mice have normal testosterone levels and only *Wnt4*-cKO males with abdominal UDT have an increase in LH and FSH levels that could be caused by the presence of atrophic testes. Given that some *Wnt4*-cKO still express WNT4 in interstitial cells, suggesting an inefficient recombination of *Rarb-cre* in these cells, the fertility defects in *Wnt4*-cKO mice could be intrinsic to the role of WNT in testicular descent. Future experiments using Leydig cell-specific KO are required to determine whether WNT4 has a role in testicular function by controlling steroidogenesis.

Estrogen exposures cause an increase in ERα distribution in the nucleus and an increase in SOX9 in the cytoplasm. These findings indicate that estrogen impacts the ability of SOX9 to translocate into the nucleus and to activate the male developmental pathway in human testicular cells (Stewart et al., 2020). *Wnt4*-cKO CDT and inguinal UDT have an increase in the number of SOX9-positive cells with SOX9 expression high in both the cytoplasm and the nucleus. This expression pattern is also seen in animal models with unilateral UDT (Moon et al., 2014). Nuclear localization of SOX9 is essential for Sertoli cell specification and testis function (Qin and Bishop, 2005; Stewart et al., 2020). The cytoplasmic retention of SOX9 in both testes of *Wnt4*-cKO mice could have disrupted Sertoli cell function, possibly inducing transcription of key ovarian genes, such as *Foxl2* and *Wnt4*, without complete sex reversal. In fact, qPCR performed on over 20 genes associated with testicular dysfunction in *Wnt4*-cKO testes revealed an upregulation of genes essential for female gonad development and function, such as *Rspo1*, *Wnt4* and *Foxl2*, in both CDT and UDT. *Foxl2*, *Rspo1*, *Ctnnb1* and *Wnt4* are known to work synergistically and in parallel to ensure proper ovarian development (Chassot et al., 2008; Ottolenghi et al., 2007; Vainio et al., 1999). In addition, they repress testis-specific genes. For example, *Foxl2* plays a crucial role in maintenance of granulosa cells and female fertility after fetal sex determination (Uhlenhaut et al., 2009). However, *Foxl2* is upregulated in testicular tumors, suggesting a common origin between Sertoli and granulosa cells (Boyer et al., 2009; Hersmus et al., 2008; Kalfa et al., 2008). We have recently demonstrated that modulation of WNT4 expression in testes is required for male fertility (Jorgez et al., 2021). The dynamics of the specific and independent actions of SOX9, ERα and WNT4 during gonadal differentiation have been well documented (Pask et al., 2010; Stewart et al., 2020; Tang et al., 2020). Our study suggests that WNT4 could have a non-cell-autonomous effect on the testicular expression of SOX9 and ERα. Future experiments are required to understand the interplay between WNT4 and SOX9. This is especially important given the observation that sex-determining genes, such as WNT4 and SOX9, remain in a steady state and are regulated by an epigenetic mechanism that can be activated later in development as a result of epigenetic memory (Garcia-Moreno et al., 2019).

In conclusion, our results indicate that the activity of WNT4 is important in the gubernaculum for the descent of the testis (Fig. 10). Although we have not determined whether the fertility defect is completely due to the role of WNT4 in testicular descent or steroidogenesis, we have found that molecular alterations also occur in the CDT of a unilaterally cryptorchid male and can impact fertility potential. Disorders of sexual development, such as UDT, can have long-lasting consequences for patients and may carry a significant risk of infertility despite early surgical intervention. This work highlights the role of the WNT4 signaling pathway in regulating testicular symmetry, descent and function. Understanding how somatic defects drive UDT, and eventually lead to azoospermia, will provide new therapeutic paradigms for boys with cryptorchidism.

MATERIALS AND METHODS
Generation of mice
All experiments were approved by The Institutional Animal Care and Use Committee (IACUC) at Baylor College of Medicine. To study the role of *Wnt4* in testicular descent, a Cre-loxP approach was used with mice previously generated and characterized by Dr Richard Behringer (Kobayashi et al., 2011). The *Wnt4*^{fl/fl} mice (Kobayashi et al., 2011) were crossed with retinoic acid receptor β2 (*Rarb*) *cre* mice (Kobayashi et al., 2005) to generate *Wnt4*[fl/fl;cre+] (*Wnt4*-cKO). *Wnt4*-cKO mice were viable at the expected Mendelian rate. *Rarb-cre* mice were crossed with the reporter line *Gt(ROSA)26Sor*[tm14(CAG-tdTomato)Hze] (Madisen et al., 2010) to determine *Rarb-cre* expression in adult tissues.

Hormone profiling
Blood samples were obtained from mice after cardiac puncture of individually housed male mice that had been in a female-free environment for 2 weeks. Blood was centrifuged at 200 *g* for 10 min in a BD-Microtainer gold tube (BD Biosciences, 365967). Serum was frozen and sent to the Ligand Assay & Analysis Core (Center for Research in Reproduction, University of Virginia Health System, VA, USA). Circulating testosterone, LH and FSH were measured according to their website (https://med.virginia.edu/research-in-reproduction/ligand-assay-analysis-core).

Fertility testing
Fertility was assessed by breeding eight *Wnt4*-cKO males to WT C57BL/6J females for 6 months and comparing litter size, number and frequency between these groups. After 6 months of mating, male mice were euthanized. Mouse body and organ weights were recorded and analyzed. Testes, epididymides and gubernacula were dissected, photographed, weighed and preserved.

Testis histology and immunohistochemistry
Testes were placed in Bouin's solution (RICCA Chemical Company, 1120-32) for 5 h at room temperature for fixation and then transferred to 70% ethanol before dehydration and paraffin embedding. Left and right testis were embedded separately. Tissue was sectioned at 5 μm. Periodic acid–Schiff (PAS) staining was performed by the Pathology Core and Lab at Baylor College of Medicine. We performed immunohistochemistry as follows. Sections were deparaffinized, and antigens were retrieved for 10 min in 10 mM sodium citrate buffer (pH 6). Slides were incubated in 3% hydrogen peroxide in PBS for 10 min to neutralize endogenous peroxidase. Sections were blocked using 2.5% horse serum (Vector Laboratories, S-2000). Primary antibodies were incubated overnight for 90 min at room temperature. Primary antibodies and dilutions were as follows: anti-CCND1 (1:100; Abcam, 133327), anti-KI67 (1:80; Abcam, 16667), anti-SOX9 (1:100; Abcam, 185230), anti-PLZF (1:100; R&D Systems, AF2944), anti-ERα (1:150; Millipore, 04820), anti-mCherry (1:500; Novus Biologicals, NBP1-96752) and anti-3β-HSD (1:200; Santa Cruz Biotechnology, 30820). Antibody detection was achieved using the ImmPRESS Horseradish Peroxidase (HRP) Polymer Reagents (Vector Laboratories, MP-7401 for rabbit antibodies and MP-7405 for goat antibodies). Finally, 3,3′-diaminobenzidine (DAB) staining was performed [SK-4100, DAB peroxidase (HRP) Substrate Kit (with Nickel)] as per manufacturer's
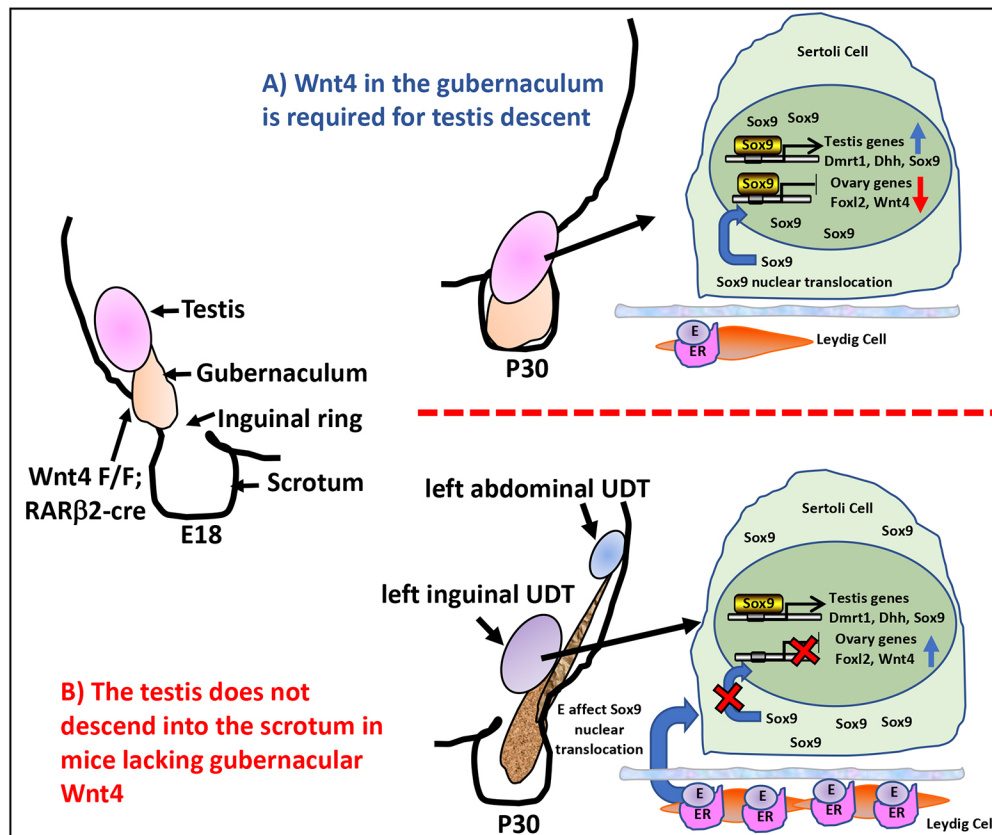
Fig. 10. Model for testicular dysfunction in *Wnt4*-cKO mice. (A) In normal conditions, gubernacular WNT4 is required for the testis to descend in the scrotum. In the descended testis, there is limited expression of estrogen (E) and activated estrogen receptors (ERs). Nuclear translocation of SOX9 in Sertoli cells occurs freely, causing the increased expression of its own gene and its downstream targets, such as *Dmrt1* and *Dhh*. (B) In mice lacking WNT4 in the gubernaculum, the left testis does not descend into the scrotum and could be located in the inguinal canal or in the abdominal cavity. The testis of *Wnt4*-cKO seems to have increased ERα and female gonadal genes, such as WNT4 and FOXL2. Recently, it was shown that estrogen action, through the binding of ERα, regulates SOX9 in Sertoli cells by blocking SOX9 nuclear translocation. A consequent increase in cytoplasmic SOX9 prevents the activation of downstream targets of SOX9 and promotes the expression of WNT4 and FOXL2 (Stewart et al., 2020). We propose that ER activation in *Wnt4*-cKO testis could inhibit SOX9 nuclear translocation in Sertoli cells and cause a decrease in male genes, such as *Dmrt1* and *Dhh*, and allow for the expression of female genes, such as *Wnt4*, *Rspo1* and *Foxl2*. P, postnatal day.

instructions. Slides were counterstained with Mayer's Hematoxylin solution (Sigma-Aldrich, MHS16). Five WT males, and five *Wnt4*-cKO with inguinal UDT and five *Wnt4*-cKO with abdominal UDT were analyzed. From each animal, at least 50 seminiferous tubules in different stages were counted. The sections were examined using an Olympus BX51 microscope and its associated software cellSens (Olympus). For WT mice, the left and right testes appeared identical. Although both testes were tested in most instances, a single image represents the WT right testis unless indicated. For *Wnt4*-cKO mice, there are significant differences between the left and right testis, and both testes are marked individually.

Protein quantification
For western blotting, 30 µg of protein/lane was electrophoresed on 10% SDS-PAGE gels and blotted onto PVDF membranes (Immobilon-P, EMD Millipore). For immunodetection, the following primary antibodies were used: rabbit polyclonal antibody against BMP4 (1:1000; Abcam, ab39973) and mouse monoclonal to β-actin (1:1000, Cell Signaling Technology, D6A8). Membranes were blocked and antibodies were diluted according to manufacturer's instructions. Goat anti-rabbit IgG (H+L)-HRP conjugate (1:3000; Bio-Rad, 170-6515) secondary antibodies were used as per manufacturer's instructions. For the chemiluminescence reaction, the SuperSignal™ West Pico PLUS Chemiluminescent Substrate (Thermo Fisher Scientific, 34580) was used. Western blot band intensity was analyzed using the freely available software NIH ImageJ (http://imagej.nih.gov/ij/).

Sperm analysis
The caudal epididymis was placed in 1 ml EmbryoMax HTF media (Millipore-sigma MR-070-D) and pre-warmed to 37°C for 15 min. For counting, sperm were diluted in sterile water and counted using five fields of

a hemocytometer. To measure motility, sperm were placed on a slide under a coverslip, and 200 sperm were counted and characterized as motile or non-motile. Counts were performed in triplicate.

qPCR
RNA was extracted using the RNeasy micro kit (QIAGEN, 74004). cDNA was prepared using the High-Capacity Reverse Transcription kit (Applied Biosystems, 4368813). Real-time PCR was performed using the following Taqman gene expression assays in which primers and probes span different exons of the mouse genes, thus excluding the possibility of genomic DNA amplification: *Ar* (Mm00442691_m1), *Ccndbp1* (Mm00487558_m1), *Bcl2* (Mm00477631_m1), *Bmp4* (Mm00432087_m1), *Ccnd1* (Mm00432459_m1), *Ccnd2* (Mm00438070_m1), *Ctnnb1* (Mm00483039_m1), *Cyp17a1* (Mm00484040_m1), *Dhh* (Mm03053542_s1), *Dmrt1* (Mm00443809_m1), *E2f1* (Mm00432939_m1), *Foxl2* (Mm00843544_s1), *Fst* (Mm00514982_m1), *Fzd4* (Mm00433382_m1), *Trp53* (Mm01731290_g1), *Gsk3b* (Mm00444911_m1), *Wnt5a* (Mm00437347_m1), *Wnt4* (Mm00437342_g1), *Zbtb16* (Mm01176868_m1), *Wt1* (Mm01337048_m1), *Sox9* (Mm00448840_m1), *Cyp19a1* (Mm00484049_m1), *Gdnf* (Mm00599849_m1), *Amh* (Mm01172800_g1), *Lgr8* (Mm00446529_m1), *Lhcgr* (Mm00442931_m1), *Rspo1* (Mm00507078_g1). The qPCR reaction was performed in a total reaction volume of 20 µl containing 1×TaqMan Universal PCR Master Mix and 1×TaqMan Gene Expression Assay Mix (thermal cycling conditions: 50°C for 2 min, 95°C for 10 min, 40 cycles at 95°C for 15 s and 60°C for 1 min). Values were normalized to *Gapdh* (Mm99999915_g1) (Applied Biosystems). Each reaction plate contained non-template controls that did not show any amplification. Plates were run and analyzed in the QuantStudio 12K Flex Real-Time PCR System to obtain the threshold cycle (C_t). The C_t is the cycle number at which the fluorescence passes a set threshold within the linear range of the amplification curves.

Quantitative analysis was conducted with RQ study software (Applied Biosystems), which uses the comparative method ($2^{-\Delta\Delta Ct}$) of relative quantification. We validated the $2^{-\Delta\Delta Ct}$ method, comparing the amplification efficiencies of complementary DNA dilutions of the target gene and internal control (*GAPDH*). Statistical analyses were made using the randomization test of the Relative Expression Software Tool (REST) from QIAGEN to indicate significance.

Selection of study patients

This study was approved by and conducted under the oversight of the Institutional Review Board of Baylor College of Medicine, Houston, TX, USA, which included a waiver of consent for a retrospective review of a large cohort of clinical genomic data. A cohort of over 17,000 individuals undergoing clinical ES at the Baylor Genetics (BG) Laboratory (Yang et al., 2014) were examined for all identified variants in *WNT4*. The ES protocol, which included library construction, exome capture by VCRome version 2.1, and HiSeq next-generation sequencing and data analysis was developed by the Human Genome Sequencing Center at Baylor College of Medicine and adapted for the clinical test of ES (Bainbridge et al., 2011; Reid et al., 2014). Individuals in this group have diverse clinical manifestations, but most often have nervous system dysfunction such as developmental delay (Yang et al., 2014). Bioinformatics assessment to determine the potential pathogenicity of the mutation was performed using PolyPhen-2 (Adzhubei et al., 2010), SIFT-PROVEAN (Choi and Chan, 2015) and MutationTaster (Schwarz et al., 2010).

WNT4 model

The homology model of WNT4 was built on the SWISS-MODEL server (swissmodel.expasy.org) using chain B of the crystal structure of the human WNT3/mouse frizzled 8 CRD (PDB ID: 6AHY) as the template (Hirai et al., 2019). The structure of WNT4 was superimposed onto the WNT3/frizzled 8 CRD complex. Sequence alignment of human WNT4 and human WNT3 was carried out using Jalview (Waterhouse et al., 2009). WNT4 shares 51.46% sequence homology with WNT3. The mutations in WNT4 were manually built and examined using the program Coot (Emsley et al., 2010). Structural figures were prepared in UCSF Chimera (Pettersen et al., 2004).

Competing interests

The Department of Molecular and Human Genetics at Baylor College of Medicine derives revenue from clinical genetic testing offered through Baylor Genetics Laboratories.

Author contributions

Conceptualization: A.S., J.C.B., C.J.J.; Methodology: A.S., J.C.B., O.M.-M., A.R., J.M., H.F., J.A.R., L.H., C.J.J.; Software: C.J.J.; Validation: A.S., J.C.B., A.R., J.M., H.F., J.A.R., L.H., C.J.J.; Formal analysis: A.S., J.C.B., O.M.-M., A.R., J.M., H.F., J.A.R., L.H., C.J.J.; Investigation: A.S., J.A.R., L.H., C.J.J.; Resources: A.S., C.J.J.; Data curation: A.S., J.C.B., O.M.-M., A.R., J.M., H.F., J.A.R., L.H., C.J.J.; Writing - original draft: A.S., J.C.B., O.M.-M., A.R., J.M., J.A.R., L.H., C.J.J.; Writing - review & editing: A.S., J.C.B., O.M.-M., A.R., J.M., H.F., J.A.R., L.H., C.J.J.; Visualization: A.S., J.C.B., A.R., J.M., H.F., J.A.R., L.H., C.J.J.; Supervision: A.S., J.C.B., C.J.J.; Project administration: A.S., J.C.B., C.J.J.; Funding acquisition: A.S., C.J.J.

References

Adzhubei, I. A., Schmidt, S., Peshkin, L., Ramensky, V. E., Gerasimova, A., Bork, P., Kondrashov, A. S. and Sunyaev, S. R. (2010). A method and server for predicting damaging missense mutations. *Nat. Methods* **7**, 248-249. doi:10.1038/nmeth0410-248

Bainbridge, M. N., Wang, M., Wu, Y., Newsham, I., Muzny, D. M., Jefferies, J. L., Albert, T. J., Burgess, D. L. and Gibbs, R. A. (2011). Targeted enrichment beyond the consensus coding DNA sequence exome reveals exons with higher variant densities. *Genome Biol.* **12**, R68. doi:10.1186/gb-2011-12-7-r68

Banerjee, A., Anjum, S., Verma, R. and Krishna, A. (2012). Alteration in expression of estrogen receptor isoforms alpha and beta, and aromatase in the testis and its relation with changes in nitric oxide during aging in mice. *Steroids* **77**, 609-620. doi:10.1016/j.steroids.2012.02.004

Barbotin, A.-L., Dauvergne, A., Dumont, A., Ramdane, N., Mitchell, V., Rigot, J.-M., Boitrelle, F. and Robin, G. (2019). Bilateral versus unilateral cryptorchidism in nonobstructive azoospermia: testicular sperm extraction outcomes. *Asian J. Androl.* **21**, 445-451. doi:10.4103/aja.aja_2_19

Barthold, J. S., Reinhardt, S. and Thorup, J. (2016). Genetic, maternal, and environmental risk factors for cryptorchidism: an update. *Eur. J. Pediatr. Surg.* **26**, 399-408. doi:10.1055/s-0036-1592416

Beumer, T. L., Roepers-Gajadien, H. L., Gademan, I. S., Kal, H. B. and de Rooij, D. G. (2000). Involvement of the D-type cyclins in germ cell proliferation and differentiation in the mouse. *Biol. Reprod.* **63**, 1893-1898. doi:10.1095/biolreprod63.6.1893

Biason-Lauber, A., Konrad, D., Navratil, F. and Schoenle, E. J. (2004). A WNT4 mutation associated with Müllerian-duct regression and virilization in a 46,XX woman. *N. Engl. J. Med.* **351**, 792-798. doi:10.1056/NEJMoa040533

Biason-Lauber, A., De Filippo, G., Konrad, D., Scarano, G., Nazzaro, A. and Schoenle, E. J. (2007). WNT4 deficiency–a clinical phenotype distinct from the classic Mayer-Rokitansky-Kuster-Hauser syndrome: a case report. *Hum. Reprod.* **22**, 224-229. doi:10.1093/humrep/del360

Boyer, A., Paquet, M., Lague, M.-N., Hermo, L. and Boerboom, D. (2009). Dysregulation of WNT/CTNNB1 and PI3K/AKT signaling in testicular stromal cells causes granulosa cell tumor of the testis. *Carcinogenesis* **30**, 869-878. doi:10.1093/carcin/bgp051

Boyer, A., Lapointe, E., Zheng, X., Cowan, R. G., Li, H., Quirk, S. M., DeMayo, F. J., Richards, J. S. and Boerboom, D. (2010). WNT4 is required for normal ovarian follicle development and female fertility. *FASEB J.* **24**, 3010-3025. doi:10.1096/fj.09-145789

Chassot, A.-A., Ranc, F., Gregoire, E. P., Roepers-Gajadien, H. L., Taketo, M. M., Camerino, G., de Rooij, D. G., Schedl, A. and Chaboissier, M.-C. (2008). Activation of beta-catenin signaling by Rspo1 controls differentiation of the mammalian ovary. *Hum. Mol. Genet.* **17**, 1264-1277. doi:10.1093/hmg/ddn016

Chen, C. H., Bournat, J. C., Wilken, N., Rosenfeld, J. A., Zhang, J., Seth, A. and Jorgez, C. J. (2020). Variants in ALX4 and their association with genitourinary defects. *Andrology* **8**, 1243-1255. doi:10.1111/andr.12815

Choi, Y. and Chan, A. P. (2015). PROVEAN web server: a tool to predict the functional effect of amino acid substitutions and indels. *Bioinformatics* **31**, 2745-2747. doi:10.1093/bioinformatics/btv195

Chung, E. and Brock, G. B. (2011). Cryptorchidism and its impact on male fertility: a state of art review of current literature. *Can. Urol. Assoc. J.* **5**, 210-214. doi:10.5489/cuaj.1010

Desgrange, A., Le Garrec, J.-F. and Meilhac, S. M. (2018). Left-right asymmetry in heart development and disease: forming the right loop. *Development* **145**, dev162776. doi:10.1242/dev.162776

Docampo, M. J. and Hadziselimovic, F. (2015). Molecular pathology of cryptorchidism-induced infertility. *Sex. Dev.* **9**, 269-278. doi:10.1159/000442059

Emsley, P., Lohkamp, B., Scott, W. G. and Cowtan, K. (2010). Features and development of Coot. *Acta Crystallogr. D Biol. Crystallogr.* **66**, 486-501. doi:10.1107/S0907444910007493

Favorito, L. A. and Sampaio, F. J. B. (2014). Testicular migration chronology: do the right and the left testes migrate at the same time? Analysis of 164 human fetuses. *BJU Int.* **113**, 650-653. doi:10.1111/bju.12574

Feng, S., Ferlin, A., Truong, A., Bathgate, R., Wade, J. D., Corbett, S., Han, S., Tannour-Louet, M., Lamb, D. J., Foresta, C. et al. (2009). INSL3/RXFP2 signaling in testicular descent. *Ann. N. Y. Acad. Sci.* **1160**, 197-204. doi:10.1111/j.1749-6632.2009.03841.x

Ferguson, L., How, J. J. and Agoulnik, A. I. (2013). The fate of spermatogonial stem cells in the cryptorchid testes of RXFP2 deficient mice. *PLoS ONE* **8**, e77351. doi:10.1371/journal.pone.0077351

Ferlin, A., Zuccarello, D., Zuccarello, B., Chirico, M. R., Zanon, G. F. and Foresta, C. (2008). Genetic alterations associated with cryptorchidism. *JAMA* **300**, 2271-2276. doi:10.1001/jama.2008.668

Ferlin, A., Zuccarello, D., Garolla, A., Selice, R., Vinanzi, C., Ganz, F., Zanon, G. F., Zuccarello, B. and Foresta, C. (2009). Mutations in INSL3 and RXFP2 genes in cryptorchid boys. *Ann. N. Y. Acad. Sci.* **1160**, 213-214. doi:10.1111/j.1749-6632.2008.03784.x

Feyles, F., Peiretti, V., Mussa, A., Manenti, M., Canavese, F., Cortese, M. G. and Lala, R. (2014). Improved sperm count and motility in young men surgically treated for cryptorchidism in the first year of life. *Eur. J. Pediatr. Surg.* **24**, 376-380. doi:10.1055/s-0033-1349715

Garcia-Moreno, S. A., Lin, Y.-T., Futtner, C. R., Salamone, I. M., Capel, B. and Maatouk, D. M. (2019). CBX2 is required to stabilize the testis pathway by repressing Wnt signaling. *PLoS Genet.* **15**, e1007895. doi:10.1371/journal.pgen.1007895

Grady, R. W., Mitchell, M. E. and Carr, M. C. (1998). Laparoscopic and histologic evaluation of the inguinal vanishing testis. *Urology* **52**, 866-869. doi:10.1016/S0090-4295(98)00326-4

Hadziselimovic, F. and Herzog, B. (2001a). The importance of both an early orchidopexy and germ cell maturation for fertility. *Lancet* **358**, 1156-1157. doi:10.1016/S0140-6736(01)06274-2

Hadziselimovic, F. and Herzog, B. (2001b). Importance of early postnatal germ cell maturation for fertility of cryptorchid males. *Horm. Res.* **55**, 6-10. doi:10.1159/000049956

Hadziselimovic, F., Hadziselimovic, N. O., Demougin, P. and Oakeley, E. J. (2011). Testicular gene expression in cryptorchid boys at risk of azoospermia. *Sex. Dev.* **5**, 49-59. doi:10.1159/000323955

Hendee, K. E., Sorokina, E. A., Muheisen, S. S., Reis, L. M., Tyler, R. C., Markovic, V., Cuturilo, G., Link, B. A. and Semina, E. V. (2018). PITX2 deficiency and associated human disease: insights from the zebrafish model. *Hum. Mol. Genet.* **27**, 1675-1695. doi:10.1093/hmg/ddy074

Hersmus, R., Kalfa, N., de Leeuw, B., Stoop, H., Oosterhuis, J. W., de Krijger, R., Wolffenbuttel, K. P., Drop, S. L. S., Veitia, R. A., Fellous, M. et al. (2008). FOXL2 and SOX9 as parameters of female and male gonadal differentiation in patients with various forms of disorders of sex development (DSD). *J. Pathol.* **215**, 31-38. doi:10.1002/path.2335

Hildorf, S., Dong, L., Thorup, J., Clasen-Linde, E., Yding Andersen, C. and Cortes, D. (2019). Sertoli cell number correlates with serum Inhibin B in infant cryptorchid boys. *Sex. Dev.* **13**, 74-82. doi:10.1159/000497374

Hirai, H., Matoba, K., Mihara, E., Arimori, T. and Takagi, J. (2019). Crystal structure of a mammalian Wnt-frizzled complex. *Nat. Struct. Mol. Biol.* **26**, 372-379. doi:10.1038/s41594-019-0216-z

Hsieh, M., Johnson, M. A., Greenberg, N. M. and Richards, J. A. S. (2002). Regulated expression of Wnts and Frizzleds at specific stages of follicular development in the rodent ovary. *Endocrinology* **143**, 898-908. doi:10.1210/endo.143.3.8684

Hutson, J. M. and Hasthorpe, S. (2005). Abnormalities of testicular descent. *Cell Tissue Res.* **322**, 155-158. doi:10.1007/s00441-005-1126-4

Hutson, J. M., Li, R., Southwell, B. R., Newgreen, D. and Cousinery, M. (2015). Regulation of testicular descent. *Pediatr. Surg. Int.* **31**, 317-325. doi:10.1007/s00383-015-3673-4

Jameson, S. A., Lin, Y.-T. and Capel, B. (2012). Testis development requires the repression of Wnt4 by Fgf signaling. *Dev. Biol.* **370**, 24-32. doi:10.1016/j.ydbio.2012.06.009

Jarow, J. P., Espeland, M. A. and Lipshultz, L. I. (1989). Evaluation of the azoospermic patient. *J. Urol.* **142**, 62-65. doi:10.1016/S0022-5347(17)38662-7

Jeays-Ward, K., Hoyle, C., Brennan, J., Dandonneau, M., Alldus, G., Capel, B. and Swain, A. (2003). Endothelial and steroidogenic cell migration are regulated by WNT4 in the developing mammalian gonad. *Development* **130**, 3663-3670. doi:10.1242/dev.00591

Jeays-Ward, K., Dandonneau, M. and Swain, A. (2004). Wnt4 is required for proper male as well as female sexual development. *Dev. Biol.* **276**, 431-440. doi:10.1016/j.ydbio.2004.08.049

Jordan, B. K., Shen, J. H.-C., Olaso, R., Ingraham, H. A. and Vilain, E. (2003). Wnt4 overexpression disrupts normal testicular vasculature and inhibits testosterone synthesis by repressing steroidogenic factor 1/β-catenin synergy. *Proc. Natl. Acad. Sci. USA* **100**, 10866-10871. doi:10.1073/pnas.1834480100

Jorgez, C. J., Seth, A., Wilken, N., Bournat, J. C., Chen, C. H. and Lamb, D. J. (2021). E2F1 regulates testicular descent and controls spermatogenesis by influencing WNT4 signaling. *Development* **148**, dev191189. doi:10.1242/dev.191189

Kaftanovskaya, E. M., Feng, S., Huang, Z., Tan, Y., Barbara, A. M., Kaur, S., Truong, A., Gorlov, I. P. and Agoulnik, A. I. (2011). Suppression of insulin-like3 receptor reveals the role of β-catenin and Notch signaling in gubernaculum development. *Mol. Endocrinol.* **25**, 170-183. doi:10.1210/me.2010-0330

Kaftanovskaya, E. M., Huang, Z., Barbara, A. M., De Gendt, K., Verhoeven, G., Gorlov, I. P. and Agoulnik, A. I. (2012). Cryptorchidism in mice with an androgen receptor ablation in gubernaculum testis. *Mol. Endocrinol.* **26**, 598-607. doi:10.1210/me.2011-1283

Kaftanovskaya, E. M., Neukirchner, G., Huff, V. and Agoulnik, A. I. (2013). Left-sided cryptorchidism in mice with Wilms' tumour 1 gene deletion in gubernaculum testis. *J. Pathol.* **230**, 39-47. doi:10.1002/path.4161

Kalfa, N., Fellous, M., Boizet-Bonhoure, B., Patte, C., Duvillard, P., Pienkowski, C., Jaubert, F., Ecochard, A. and Sultan, C. (2008). Aberrant expression of ovary determining gene FOXL2 in the testis and juvenile granulosa cell tumor in children. *J. Urol.* **180**, 1810-1813. doi:10.1016/j.juro.2008.03.097

Kiewisz, J., Skowronska, A., Winiarska, A., Pawlowska, K., Kiezun, J., Rozicka, A., Perkowska-Ptasinska, A., Kmiec, Z. and Stompor, T. (2019). WNT4 expression in primary and secondary kidney diseases: dependence on staging. *Kidney Blood Press. Res.* **44**, 200-210. doi:10.1159/000498989

Kobayashi, A., Kwan, K.-M., Carroll, T. J., McMahon, A. P., Mendelsohn, C. L. and Behringer, R. R. (2005). Distinct and sequential tissue-specific activities of the LIM-class homeobox gene Lim1 for tubular morphogenesis during kidney development. *Development* **132**, 2809-2823. doi:10.1242/dev.01858

Kobayashi, A., Stewart, C. A., Wang, Y., Fujioka, K., Thomas, N. C., Jamin, S. P. and Behringer, R. R. (2011). β-Catenin is essential for Mullerian duct regression during male sexual differentiation. *Development* **138**, 1967-1975. doi:10.1242/dev.056143

Kollin, C., Stukenborg, J. B., Nurmio, M., Sundqvist, E., Gustafsson, T., Söder, O., Toppari, J., Nordenskjöld, A. and Ritzen, E. M. (2012). Boys with undescended testes: endocrine, volumetric and morphometric studies on testicular function before and after orchidopexy at nine months or three years of age. *J. Clin. Endocrinol. Metab.* **97**, 4588-4595. doi:10.1210/jc.2012-2325

Kolon, T. F., Anthony Herndon, C. D., Baker, L. A., Baskin, L. S., Baxter, C. G., Cheng, E. Y., Diaz, M., Lee, P. A., Seashore, C. J., Tasian, G. E. et al. (2014). Evaluation and treatment of cryptorchidism: AUA guideline. *J. Urol.* **192**, 337-345. doi:10.1016/j.juro.2014.05.005

Komarowska, M. D., Hermanowicz, A. and Debek, W. (2015). Putting the pieces together: cryptorchidism - do we know everything? *J. Pediatr. Endocrinol. Metab.* **28**, 1247-1256. doi:10.1515/jpem-2015-0098

Kuroda, J., Nakamura, M., Yoshida, M., Yamamoto, H., Maeda, T., Taniguchi, K., Nakazawa, N., Hatori, R., Ishio, A., Ozaki, A. et al. (2012). Canonical Wnt signaling in the visceral muscle is required for left-right asymmetric development of the Drosophila midgut. *Mech. Dev.* **128**, 625-639. doi:10.1016/j.mod.2011.12.002

Lee, P. A., O'Leary, L. A., Songer, N. J., Coughlin, M. T., Bellinger, M. F. and LaPorte, R. E. (1996). Paternity after unilateral cryptorchidism: a controlled study. *Pediatrics* **98**, 676-679. doi:10.1542/peds.98.4.676

Lee, P. A., O'Leary, L. A., Songer, N. J., Coughlin, M. T., Bellinger, M. F. and LaPorte, R. E. (1997). Paternity after bilateral cryptorchidism. A controlled study. *Arch. Pediatr. Adolesc. Med.* **151**, 260-263. doi:10.1001/archpedi.1997.02170400046008

Lie, G. and Hutson, J. M. (2011). The role of cremaster muscle in testicular descent in humans and animal models. *Pediatr. Surg. Int.* **27**, 1255-1265. doi:10.1007/s00383-011-2983-4

Lipshultz, L. I., Caminos-Torres, R., Greenspan, C. S. and Snyder, P. J. (1976). Testicular function after orchiopexy for unilaterally undescended testis. *N. Engl. J. Med.* **295**, 15-18. doi:10.1056/NEJM197607012950104

Madisen, L., Zwingman, T. A., Sunkin, S. M., Oh, S. W., Zariwala, H. A., Gu, H., Ng, L. L., Palmiter, R. D., Hawrylycz, M. J., Jones, A. R. et al. (2010). A robust and high-throughput Cre reporting and characterization system for the whole mouse brain. *Nat. Neurosci.* **13**, 133-140. doi:10.1038/nn.2467

Mandel, H., Shemer, R., Borochowitz, Z. U., Okopnik, M., Knopf, C., Indelman, M., Drugan, A., Tiosano, D., Gershoni-Baruch, R., Choder, M. et al. (2008). SERKAL syndrome: an autosomal-recessive disorder caused by a loss-of-function mutation in WNT4. *Am. J. Hum. Genet.* **82**, 39-47. doi:10.1016/j.ajhg.2007.08.005

Markewitz, M., Lattimer, J. K. and Veenema, R. J. (1970). A comparative study of germ cell kinetics in the testes of children with unilateral cryptorchidism: a preliminary report. *Fertil. Steril.* **21**, 806-815. doi:10.1016/S0015-0282(16)37867-0

Matsuyama, M., Haneda, C. and Kato, K. (2013). Congenic strain differences of renal malformations in ACI/Mna rats by introgression of the chromosomal region of BUF/Mna rats containing Pur1. *Nagoya J. Med. Sci.* **75**, 251-254.

Minegishi, K., Hashimoto, M., Ajima, R., Takaoka, K., Shinohara, K., Ikawa, Y., Nishimura, H., McMahon, A. P., Willert, K., Okada, Y. et al. (2017). A Wnt5 activity asymmetry and intercellular signaling via PCP proteins polarize node cells for left-right symmetry breaking. *Dev. Cell* **40**, 439-452.e434. doi:10.1016/j.devcel.2017.02.010

Mizuno, K., Kojima, Y., Kurokawa, S., Kamisawa, H., Kohri, K. and Hayashi, Y. (2011). Altered expression and localization of estrogen receptors alpha and beta in the testes of a cryptorchid rat model. *Urology* **77**, 251.e251-251.e256. doi:10.1016/j.urology.2010.06.035

Moon, J. H., Yoo, D. Y., Jo, Y. K., Kim, G. A., Jung, H. Y., Choi, J. H., Hwang, I. K. and Jang, G. (2014). Unilateral cryptorchidism induces morphological changes of testes and hyperplasia of Sertoli cells in a dog. *Lab. Anim. Res.* **30**, 185-189. doi:10.5625/lar.2014.30.4.185

Nakaya, M.-A., Biris, K., Tsukiyama, T., Jaime, S., Rawls, J. A. and Yamaguchi, T. P. (2005). Wnt3a links left-right determination with segmentation and anteroposterior axis elongation. *Development* **132**, 5425-5436. doi:10.1242/dev.02149

Niewenhuis, R. J. (1980). Effect of cryptorchidism and orchidopexy on 3B hydroxysteroid dehydrogenase activity in rat testicle. *Arch. Androl.* **4**, 231-234. doi:10.3109/01485018008986968

Ottolenghi, C., Pelosi, E., Tran, J., Colombino, M., Douglass, E., Nedorezov, T., Cao, A., Forabosco, A. and Schlessinger, D. (2007). Loss of Wnt4 and Foxl2 leads to female-to-male sex reversal extending to germ cells. *Hum. Mol. Genet.* **16**, 2795-2804. doi:10.1093/hmg/ddm235

Pask, A. J., Calatayud, N. E., Shaw, G., Wood, W. M. and Renfree, M. B. (2010). Oestrogen blocks the nuclear entry of SOX9 in the developing gonad of a marsupial mammal. *BMC Biol.* **8**, 113. doi:10.1186/1741-7007-8-113

Pettersen, E. F., Goddard, T. D., Huang, C. C., Couch, G. S., Greenblatt, D. M., Meng, E. C. and Ferrin, T. E. (2004). UCSF Chimera – a visualization system for exploratory research and analysis. *J. Comput. Chem.* **25**, 1605-1612. doi:10.1002/jcc.20084

DEVELOPMENT

Philibert, P., Biason-Lauber, A., Gueorguieva, I., Stuckens, C., Pienkowski, C., Lebon-Labich, B., Paris, F. and Sultan, C. (2011). Molecular analysis of WNT4 gene in four adolescent girls with mullerian duct abnormality and hyperandrogenism (atypical Mayer-Rokitansky-Küster-Hauser syndrome). Fertil. Steril. 95, 2683-2686. doi:10.1016/j.fertnstert.2011.01.152

Pike, M. C., Chilvers, C. and Peckham, M. J. (1986). Effect of age at orchidopexy on risk of testicular cancer. Lancet 327, 1246-1248. doi:10.1016/S0140-6736(86)91389-9

Qin, Y. and Bishop, C. E. (2005). Sox9 is sufficient for functional testis development producing fertile male mice in the absence of Sry. Hum. Mol. Genet. 14, 1221-1229. doi:10.1093/hmg/ddi133

Reid, J. G., Carroll, A., Veeraraghavan, N., Dahdouli, M., Sundquist, A., English, A., Bainbridge, M., White, S., Salerno, W., Buhay, C. et al. (2014). Launching genomics into the cloud: deployment of Mercury, a next generation sequence analysis pipeline. BMC Bioinformatics 15, 30. doi:10.1186/1471-2105-15-30

Ritzén, E. M., Bergh, A., Bjerknes, R., Christiansen, P., Cortes, D., Haugen, S. E., Jörgensen, N., Kollin, C., Lindahl, S., Läckgren, G. et al. (2007). Nordic consensus on treatment of undescended testes. Acta Paediatr. 96, 638-643. doi:10.1111/j.1651-2227.2006.00159.x

Schreuder, M. F. (2011). Unilateral anomalies of kidney development: why is left not right? Kidney Int. 80, 740-745. doi:10.1038/ki.2011.204

Schreuder, M. F., Westland, R. and van Wijk, J. A. E. (2009). Unilateral multicystic dysplastic kidney: a meta-analysis of observational studies on the incidence, associated urinary tract malformations and the contralateral kidney. Nephrol. Dial. Transplant. 24, 1810-1818. doi:10.1093/ndt/gfn777

Schwarz, J. M., Rödelsperger, C., Schuelke, M. and Seelow, D. (2010). MutationTaster evaluates disease-causing potential of sequence alterations. Nat. Methods 7, 575-576. doi:10.1038/nmeth0810-575

Simonetti, G. D. and Mohaupt, M. G. (2012). Smaller left kidney in low birth weight children. Kidney Int. 81, 418; author reply 418-419. doi:10.1038/ki.2011.391

Spires, S. E., Woolums, C. S., Pulito, A. R. and Spires, S. M. (2000). Testicular regression syndrome: a clinical and pathologic study of 11 cases. Arch. Pathol. Lab. Med. 124, 694-698. doi:10.5858/2000-124-0694-TRS

Stark, K., Vainio, S., Vassileva, G. and McMahon, A. P. (1994). Epithelial transformation of metanephric mesenchyme in the developing kidney regulated by Wnt-4. Nature 372, 679-683. doi:10.1038/372679a0

Steger, K., Aleithe, I., Behre, H. and Bergmann, M. (1998). The proliferation of spermatogonia in normal and pathological human seminiferous epithelium: an immunohistochemical study using monoclonal antibodies against Ki-67 protein and proliferating cell nuclear antigen. Mol. Hum. Reprod. 4, 227-233. doi:10.1093/molehr/4.3.227

Stewart, M. K., Mattiske, D. M. and Pask, A. J. (2020). Estrogen suppresses SOX9 and activates markers of female development in a human testis-derived cell line. BMC Mol. Cell Biol. 21, 66. doi:10.1186/s12860-020-00307-9

Suomi, A.-M., Main, K. M., Kaleva, M., Schmidt, I. M., Chellakooty, M., Virtanen, H. E., Boisen, K. A., Damgaard, I. N., Kai, C. M., Skakkebæk, N. E. et al. (2006). Hormonal changes in 3-month-old cryptorchid boys. J. Clin. Endocrinol. Metab. 91, 953-958. doi:10.1210/jc.2004-2318

Suzuki, Y., Sasagawa, I., Ashida, J., Nakada, T., Muroya, K. and Ogata, T. (2001). Screening for mutations of the androgen receptor gene in patients with isolated cryptorchidism. Fertil. Steril. 76, 834-836. doi:10.1016/S0015-0282(01)02016-7

Tang, F., Richardson, N., Albina, A., Chaboissier, M.-C. and Perea-Gomez, A. (2020). Mouse gonad development in the absence of the pro-ovary factor WNT4 and the pro-testis factor SOX9. Cells 9, 1103. doi:10.3390/cells9051103

Uhlenhaut, N. H., Jakob, S., Anlag, K., Eisenberger, T., Sekido, R., Kress, J., Treier, A.-C., Klugmann, C., Klasen, C., Holter, N. I. et al. (2009). Somatic sex reprogramming of adult ovaries to testes by FOXL2 ablation. Cell 139, 1130-1142. doi:10.1016/j.cell.2009.11.021

Vaganée, D., Daems, F., Aerts, W., Dewaide, R., van den Keybus, T., De Baets, K., De Wachter, S. and De Win, G. (2018). Testicular asymmetry in healthy adolescent boys. BJU Int. 122, 654-666. doi:10.1111/bju.14174

Vainio, S., Heikkilä, M., Kispert, A., Chin, N. and McMahon, A. P. (1999). Female development in mammals is regulated by Wnt-4 signalling. Nature 397, 405-409. doi:10.1038/17068

Verkauskas, G., Malcius, D., Dasevicius, D. and Hadziselimovic, F. (2019). Histopathology of unilateral cryptorchidism. Pediatr. Dev. Pathol. 22, 53-58. doi:10.1177/1093526618789300

Virtanen, H. E. and Toppari, J. (2008). Epidemiology and pathogenesis of cryptorchidism. Hum. Reprod. Update 14, 49-58. doi:10.1093/humupd/dmm027

Vivante, A., Mark-Danieli, M., Davidovits, M., Harari-Steinberg, O., Omer, D., Gnatek, Y., Cleper, R., Landau, D., Kovalski, Y., Weissman, I. et al. (2013). Renal hypodysplasia associates with a WNT4 variant that causes aberrant canonical WNT signaling. J. Am. Soc. Nephrol. 24, 550-558. doi:10.1681/ASN.2012010097

Walentek, P., Schneider, I., Schweickert, A. and Blum, M. (2013). Wnt11b is involved in cilia-mediated symmetry breakage during Xenopus left-right development. PLoS ONE 8, e73646. doi:10.1371/journal.pone.0073646

Waterhouse, A. M., Procter, J. B., Martin, D. M. A., Clamp, M. and Barton, G. J. (2009). Jalview Version 2 – a multiple sequence alignment editor and analysis workbench. Bioinformatics 25, 1189-1191. doi:10.1093/bioinformatics/btp033

Welsh, I. C., Thomsen, M., Gludish, D. W., Alfonso-Parra, C., Bai, Y., Martin, J. F. and Kurpios, N. A. (2013). Integration of left-right Pitx2 transcription and Wnt signaling drives asymmetric gut morphogenesis via Daam2. Dev. Cell 26, 629-644. doi:10.1016/j.devcel.2013.07.019

Wiener, J. S., Marcelli, M., Gonzales, E. T., Jr, Roth, D. R. and Lamb, D. J. (1998). Androgen receptor gene alterations are not associated with isolated cryptorchidism. J. Urol. 160, 863-865. doi:10.1016/S0022-5347(01)62823-4

Yang, Y., Muzny, D. M., Xia, F., Niu, Z., Person, R., Ding, Y., Ward, P., Braxton, A., Wang, M., Buhay, C. et al. (2014). Molecular findings among patients referred for clinical whole-exome sequencing. JAMA 312, 1870-1879. doi:10.1001/jama.2014.14601

Zhao, W.-P., Wang, H.-W., Liu, J., Tan, P.-P., Luo, X.-L., Zhu, S.-Q., Chen, X.-L. and Zhou, B.-H. (2018). Positive PCNA and Ki-67 expression in the testis correlates with spermatogenesis dysfunction in fluoride-treated rats. Biol. Trace Elem. Res. 186, 489-497. doi:10.1007/s12011-018-1338-6

Zimmermann, S., Steding, G., Emmen, J. M. A., Brinkmann, A. O., Nayernia, K., Holstein, A. F., Engel, W. and Adham, I. M. (1999). Targeted disruption of the Insl3 gene causes bilateral cryptorchidism. Mol. Endocrinol. 13, 681-691. doi:10.1210/mend.13.5.0272
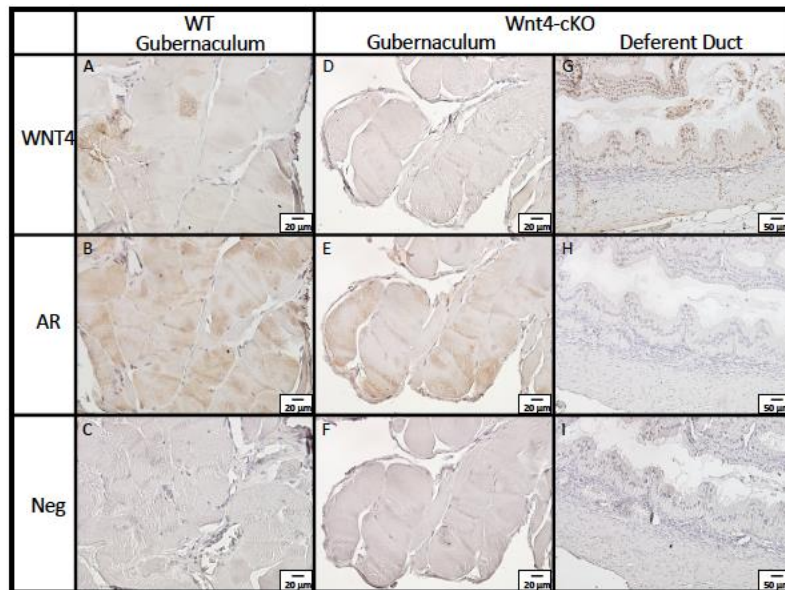
DEVELOPMENT

Fig. S1. WNT4 is not expressed in the gubernaculum of *Wnt4*-cKO mice. **A**) WNT4 (brown staining) is expressed in the adult gubernaculum of WT mice. **D, G**) In *Wnt4*-cKO mice, WNT4 has low or no expression in the gubernaculum (D), but is expressed in the deferent ducts (G). **B, E, H**) AR is expressed in the gubernaculum of WT (B) and *Wnt4*-cKO mice (E), but not in the deferent duct of *Wnt4*-cKO mice (H). **C, F, I**) Negative controls (lack of primary antibody) of WT gubernaculum (C), *Wnt4*-cKO mice gubernaculum (F), and *Wnt4*-cKO mice deferent ducts (I).
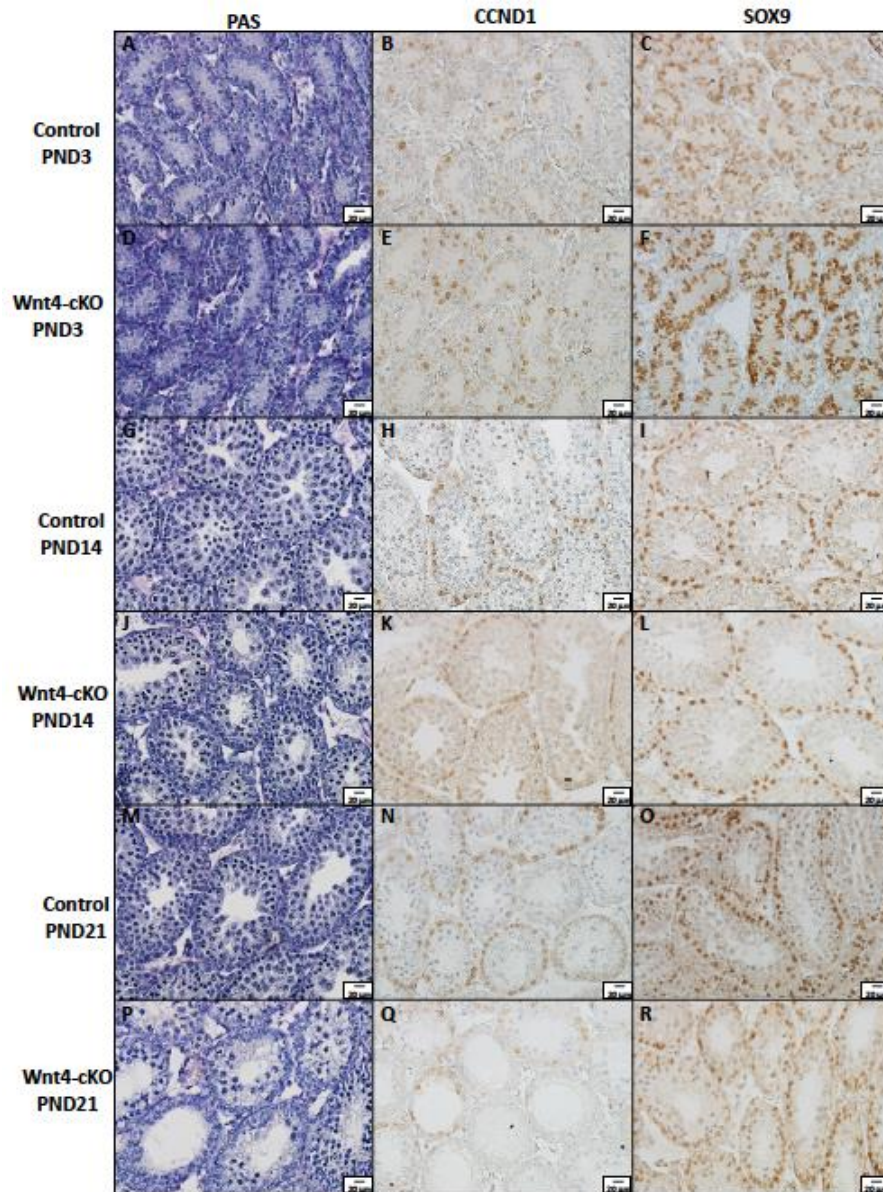
Fig. S2. Testicular morphology of *Wnt4*-cKO mice before puberty. *Wnt4*-cKO mice testes on postnatal day 3 have similar morphology [PAS staining (**D**)], distribution of CCND1 (**E**), and distribution of SOX9 positive cells (**F**) to age-matched control mice (**A-C**). *Wnt4*-cKO mice testes on postnatal day 14 have similar morphology (**J**), distribution of CCND1 (**K**), and distribution of SOX9 positive cells (**L**) to age-matched control mice (**G-I**). At puberty (postnatal day 21), some differences were observed in the left UDT of *Wnt4*-cKO mice, with seminiferous tubules (ST) lacking layers of germ cells (**P**) when compared to age-matched control mice (**M**). The ST of *Wnt4*-cKO mice that have less cellularity also have less CCND1-positive cells (**Q**) when compared to control mice (**N**) at PND21. *Wnt4*-cKO mice testes on postnatal day 21 have similar SOX9-positive cells (**R**) when compared to age-matched control mice (**O**).
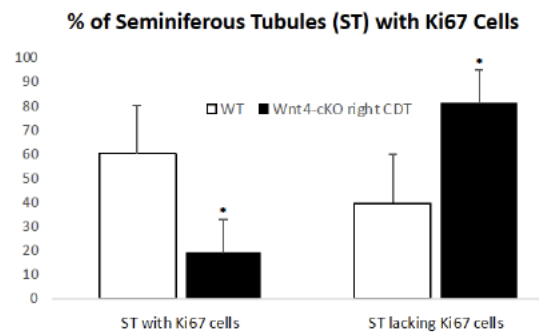
Fig. S3. *Wnt4*-cKO mice have less KI67. The number of ST per cross-section were scored for the presence or absence of KI67-positive cells in the WT right testis and the right CDT of *Wnt4*-cKO mice. 70-190 ST were counted in each mouse (n=10). The white bar indicates the percentage of ST in WT mice and the black bars indicates the percentage of ST in *Wnt4*-cKO mice. A significant difference (*p<0.001) was identified between WT and *Wnt4*-cKO CDT. Data are presented as average±SD, and were analyzed using one-way ANOVA with Bonferroni correction
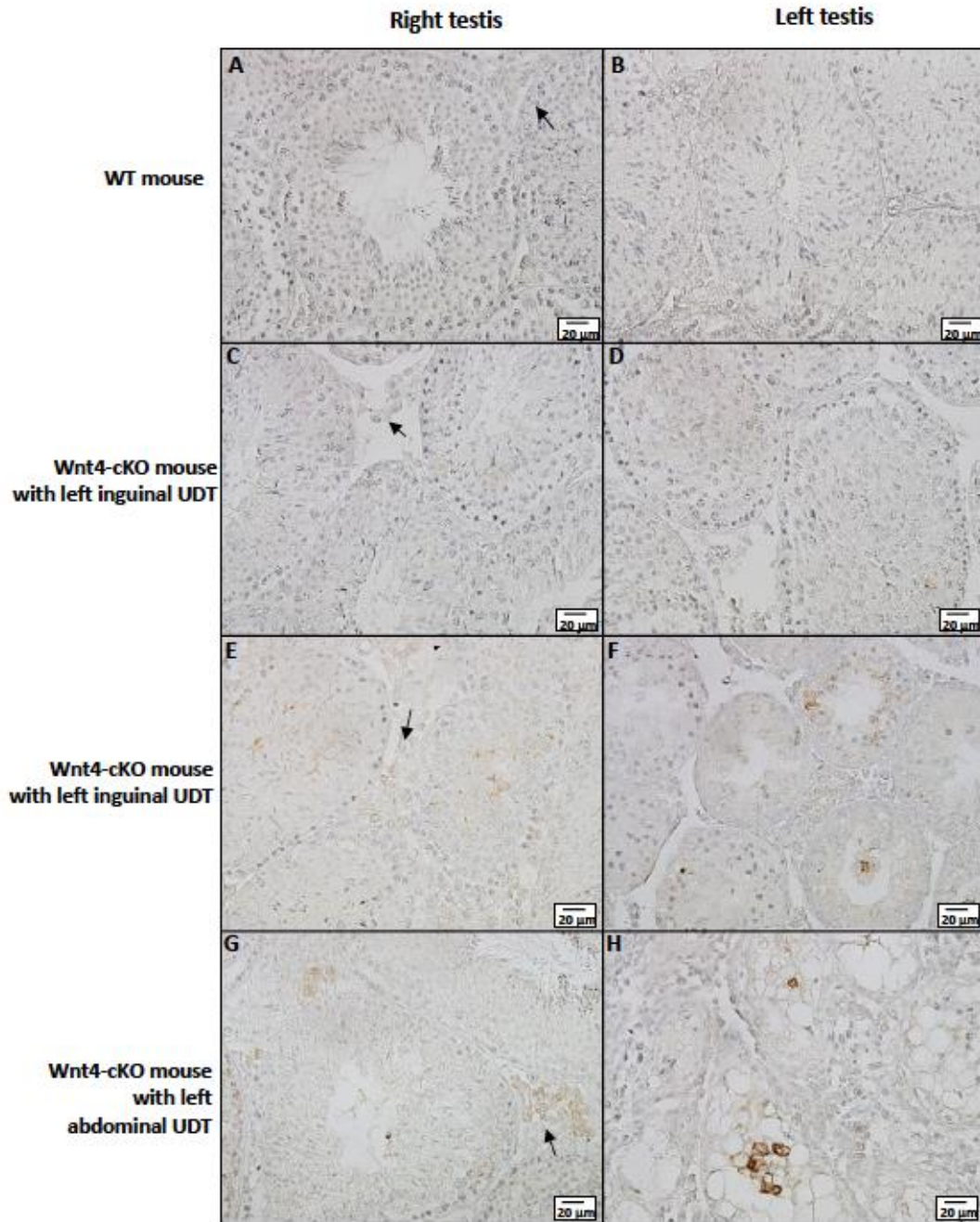
Fig. S4. WNT4 is expressed in the testis of *Wnt4*-cKO mice. Expression of WNT4 in left and right testes of WT and *Wnt4*-cKO mice. **A-B**) WNT4 is expressed in a few interstitial cells of adult mice (black arrow). **C-H**). Variability in WNT4 expression in *Wnt4*-cKO mice is observed with lack of expression in *Wnt4*-cKO mouse with left inguinal UDT (**C-D**) and expression in both interstitial (black arrow) and cells and inside the ST in *Wnt4*-cKO mouse with left inguinal UDT (**E-F**) as well as with left abdominal UDT (**G-H**).
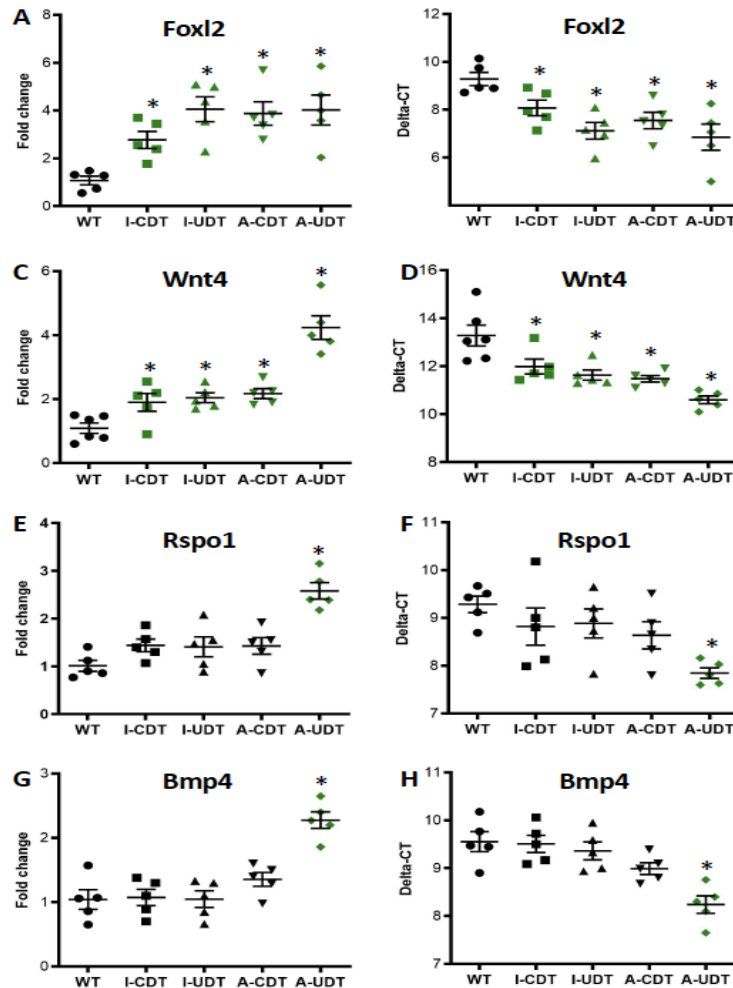
Fig. S5. Differential expression analysis of genes upregulated in the *Wnt4-cKO* mouse testes. Box plots represent the gene expression levels (Mean±SEM) of four of the most significantly upregulated genes in *Wnt4-cKO* mouse testes represented in two different ways as fold change (delta-delta-CT) and delta-CT. Five groups of mice are indicated: WT, inguinal CDT and UDT, and abdominal CDT and UDT (n=5 mice per group). **A, B**) Foxl2 levels are significantly upregulated in inguinal CDT and UDT, and abdominal CDT and UDT (green boxes). **C, D**) Wnt4 levels are significantly upregulated in inguinal CDT and UDT, and abdominal CDT and UDT (green boxes). **E, F**) Rspo1 levels are significantly upregulated in abdominal UDT (green boxes). **G, H**) Bmp4 levels are significantly upregulated in abdominal UDT (green boxes). Relative fold change of Wnt4, Foxl2, Rspo1 and Bmp4 in *Wnt4-cKO* mouse testes versus control testis was calculated using delta-delta-CT (deltaCT (a target sample) −deltaCT (a reference sample) from qPCR data. Gapdh gene was used as internal control for normalization. Data was obtained and plotted from the ExpressionSuite Software (|Log2FC| Cutoff: 1; *p value < 0.01).
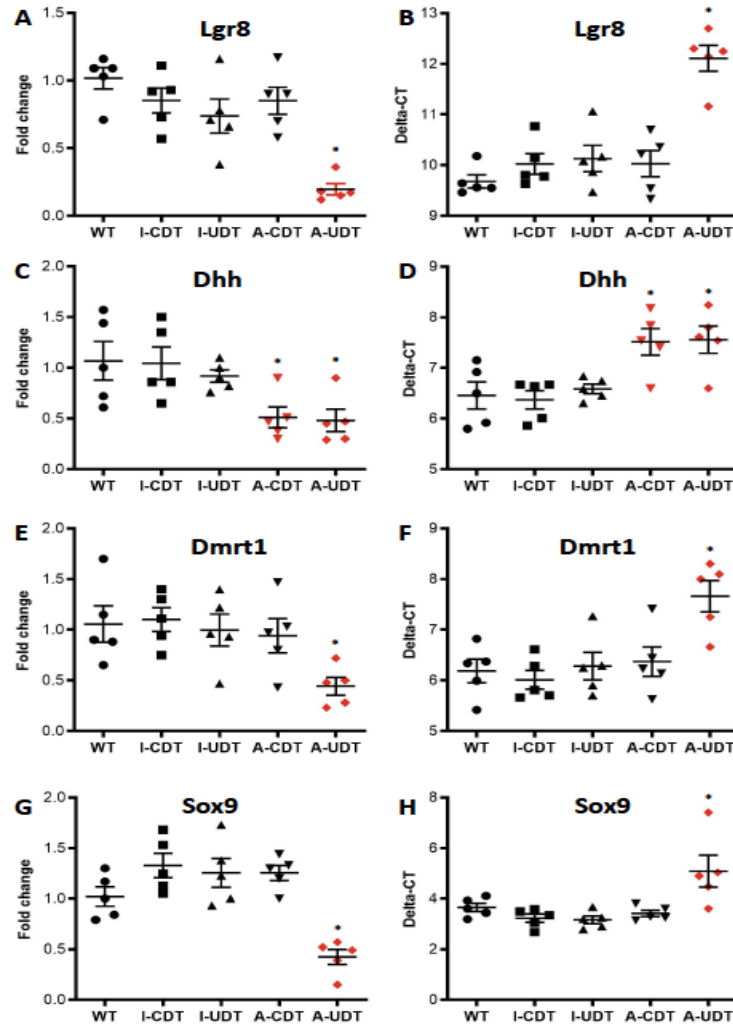
Fig. S6. Differential expression analysis of genes downregulated in the *Wnt4-cKO* mouse testes. Box plots represent the gene expression levels (Mean±SEM) of four of the most significantly downregulated genes in *Wnt4-cKO* mouse testes represented in two different ways as fold change (delta-delta-CT) and delta-CT. Five groups of mice are indicated: WT, inguinal CDT and UDT, and abdominal CDT and UDT (n=5 mice per group). **A, B**) Lgr8 levels are significantly downregulated in abdominal UDT (red boxes). **C, D**) Dhh levels are significantly downregulated in abdominal CDT and UDT (red boxes). **E, F**) Dmrt1 levels are significantly downregulated in abdominal UDT (red boxes). **G, H**) Sox9 levels are significantly downregulated in abdominal UDT (red boxes). Relative fold change of Dhh, Sox9, Lgr8 and Dmrt1 in *Wnt4-cKO* mouse testes versus control testis was calculated using delta-delta-CT (deltaCT (a target sample)−deltaCT (a reference sample)) from qPCR data. Gapdh gene was used as internal control for normalization. Data was obtained and plotted from the ExpressionSuite Software (| Log2FC| Cutoff: 1; * p value < 0.01).